Article

Current Biology

Multiple gene co-options underlie the rapid evolution of sexually deceptive flowers in *Gorteria diffusa*

Highlights

- Co-option of iron homeostasis, root hair, and phase transition genes in petal spots
- Co-options change coloration, cell structure, and placement of petal spots
- Altered petal spots mimic female flies and enable pollination by sexual deception
- Integration of multiple gene co-options facilitates the evolution of novel traits

Authors

Roman T. Kellenberger, Udhaya Ponraj, Boris Delahaie, ..., Karin H. Müller, Allan G. Ellis, Beverley J. Glover

Correspondence

rk615@cam.ac.uk (R.T.K.), bjg26@cam.ac.uk (B.J.G.)

In brief

Using an integrative evo-devo approach, Kellenberger et al. show that three independent gene co-options altering the color, structure, and placement of petal spots underlie the evolution of sexual deception in the daisy *Gorteria diffusa*. This work shows that gene co-options can combine in a modular way, giving rise to complex phenotypic novelties.

Kellenberger et al., 2023, Current Biology *33*, 1502–1512
April 24, 2023
https://doi.org/10.1016/j.cub.2023.03.003

CellPress

CellPress
OPEN ACCESS

Current Biology

Article

Multiple gene co-options underlie the rapid evolution of sexually deceptive flowers in *Gorteria diffusa*

Roman T. Kellenberger,[1,9,*] Udhaya Ponraj,[1] Boris Delahaie,[1,2,3] Róisín Fattorini,[1,4] Janneke Balk,[5,6] Sara Lopez-Gomollon,[1] Karin H. Müller,[7] Allan G. Ellis,[8] and Beverley J. Glover[1,10,11,*]

[1]Department of Plant Sciences, University of Cambridge, Downing Street, Cambridge CB2 3EA, UK
[2]CIRAD, UMR DIADE, Montpellier 34398, France
[3]UMR DIADE, Université de Montpellier, CIRAD, IRD, Montpellier, France
[4]Department of Biochemistry and Systems Biology, Institute of Systems, Molecular and Integrative Biology, University of Liverpool, Liverpool L69 7ZB, UK
[5]Department of Biochemistry and Metabolism, John Innes Centre, Norwich NR4 7UH, UK
[6]School of Biological Sciences, University of East Anglia, Norwich NR4 4JT, UK
[7]Cambridge Advanced Imaging Centre, University of Cambridge, Downing Street, Cambridge CB2 3DY, UK
[8]Department of Botany and Zoology, Stellenbosch University, Private Bag X1, Matieland 7602, South Africa
[9]Twitter: @RT_Kellenberger
[10]Twitter: @Beverley_CUBG
[11]Lead contact
*Correspondence: rk615@cam.ac.uk (R.T.K.), bjg26@cam.ac.uk (B.J.G.)
https://doi.org/10.1016/j.cub.2023.03.003

SUMMARY

Gene co-option, the redeployment of an existing gene in an unrelated developmental context, is an important mechanism underlying the evolution of morphological novelty. In most cases described to date, novel traits emerged by co-option of a single gene or genetic network. Here, we show that the integration of multiple co-opted genetic elements facilitated the rapid evolution of complex petal spots that mimic female bee-fly pollinators in the sexually deceptive South African daisy *Gorteria diffusa*. First, co-option of iron homeostasis genes altered petal spot pigmentation, producing a color similar to that of female pollinators. Second, co-option of the root hair gene *GdEXPA7* enabled the formation of enlarged papillate petal epidermal cells, eliciting copulation responses from male flies. Third, co-option of the *miR156-GdSPL1* transcription factor module altered petal spot placement, resulting in better mimicry of female flies resting on the flower. The three genetic elements were likely co-opted sequentially, and strength of sexual deception in different *G. diffusa* floral forms strongly correlates with the presence of the three corresponding morphological alterations. Our findings suggest that gene co-options can combine in a modular fashion, enabling rapid evolution of novel complex traits.

INTRODUCTION

Gene co-option, i.e., repurposing a partial or entire pre-existing genetic network in an unrelated developmental context, is a major mechanism underlying the rapid evolution of novel complex traits.[1] After co-option a genetic network often undergoes adaptive modifications, which further alter the morphology of the novel trait.[2,3] Nevertheless, the evolvability of pre-wired genetic networks is constrained,[2] and such modifications fall short in explaining more complex cases where rapidly evolved novel traits resemble either none, or combinations of several, ancestral traits. The sudden appearance of such composite novelties must thus be driven by additional molecular-developmental mechanisms, including the addition of recruited or orphan genes to co-opted gene networks,[4,5] the concurrent re-wiring of ancestral networks,[6] multiple co-options of the same network,[7] or the co-option of an overarching transcription factor (TF) network.[8,9] However, most composite novel traits investigated to date are highly derived but not recently evolved, making it difficult to discern the initial changes that gave rise to the novelty from later alterations. Understanding how composite novelties emerge within a short time requires empirical data from systems that are currently undergoing this process.

Particularly sophisticated complex traits are involved in plant sexual deception, when flowers evolve novel structures mimicking mating signals of female insects to attract males for pollination.[10] Plant sexual deception is almost exclusively confined to the Orchidaceae, where it evolved independently in several genera from different continents.[11] In orchids, sexual deception is highly efficient and specific with flowers tricking males into pseudocopulation by concurrent imitation of the appearance,[12] texture,[13] and sexual pheromones[10,14,15] of females. The molecular basis of several sexually deceptive floral structures has been described,[11,16–19] and studies have shown

CellPress
OPEN ACCESS

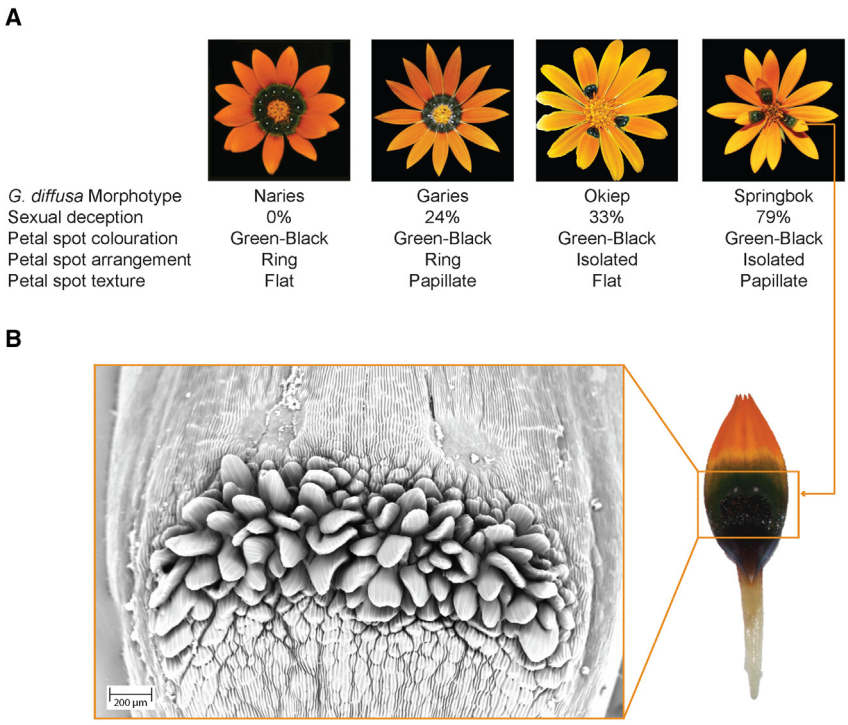

Figure 1. *Gorteria diffusa* petal spot morphology and gene expression

(A) Strength of sexual deception in *G. diffusa* morphotypes depends on coloration, arrangement, and texture of petal spots (4 out of 15 morphotypes shown).

(B) Cryoscanning electron microscopy (cryo-SEM) image of a sexually deceptive petal spot from the Springbok morphotype, consisting of a dark green-black pigmented area with a band of multicellular tongue-shaped papillae below two white UV light reflecting dots (see also Figure S1).

(C) Volcano plot depicting the result of the differential gene expression analysis. A total of 526 transcripts were differentially expressed between spotted and unspotted Springbok ray florets (|fold change| ≥ 1.5 and FDR-adjusted p value < 0.05 [dashed lines], quasi-likelihood F test). 149 of these transcripts were also differentially expressed between sexually deceptive Springbok and non-deceptive Naries spotted ray florets (triangular points, see also Figure S2). Colored points denote differentially expressed transcripts from the genetic pathways involved in petal spot pigmentation (anthocyanin biosynthesis and iron ion homeostasis), papillae formation (root development), and petal spot positioning (flowering initiation, see also Table S1).

that minor mutations in the underlying genetic networks can drastically change the effectiveness of the mimicry.[20,21] The evolution of sexually deceptive flowers thus necessitates orchestrated changes in several genetic networks altering multiple unrelated floral features, which classifies plant sexual deception as a composite novelty. There are several hypotheses on the evolutionary trajectories leading to sexually deceptive orchid flowers, for example, with simple food[22–24] or shelter mimicry[25] as an intermediate step, and recent studies suggest that evolutionary novelty[26] and gene co-option[19] played an important role in this process. However, due to the lack of intermediate, weakly sexually deceptive orchid taxa, the molecular-developmental changes underlying the evolution of plant sexual deception are largely uncharacterized.

The South African daisy *Gorteria diffusa* Thunb. (Asteraceae), a self-incompatible ephemeral herb from the winter-rainfall Namaqualand desert, is one of a handful of confirmed sexually deceptive plant species outside of the Orchidaceae.[27,28] Between 0.6 and 2.2 mya, *G. diffusa* radiated into 15 parapatric floral forms (morphotypes), which hybridize in narrow zones of secondary contact.[29] All morphotypes are pollinated by the same bombyliid fly (*Megapalpus capensis* Wiedeman) and differ mainly in number, positioning, and morphology of dark, raised petal spots on the yellow-orange ray florets (Figure 1A).[27,30] In some morphotypes, the petal spots form simple nectar-guiding rings, a widespread feature among angiosperm flowers.[31] In other morphotypes, however, the petal spots have more complex morphologies with the most elaborate ones resembling dark flies resting on the flower.[27,30] This continuum in *G. diffusa* petal spot complexity is matched by a continuum in strength of sexual deception in *M. capensis* males, ranging from normal feeding behavior to mate searching and pseudocopulation.[28,32] Sexual deception in *G. diffusa* differs from deceptive orchid systems: (1) deception of males is only based on visual and tactile stimuli without olfactory cues;[32] (2) while sexual deception enhances pollen export, all morphotypes still offer nectar to both male and female *M. capensis*;[28] (3) to our knowledge, *G. diffusa* is the only plant species where intermediate, weakly sexually deceptive forms still exist. Considering the young age of the group, these aspects suggest that sexually deceptive petal spots in *G. diffusa* evolved recently and rapidly, and deceptive pollination does not (yet) fully replace the ancestral rewarding pollination.

Here, we use an evo-devo approach to study the molecular changes underlying the evolution of sexual deception in

G. diffusa. Previous studies identified three main petal spot components involved in sexual deception (Figures 1A, 1B, and S1): (1) green-black pigment around UV reflective white dots imitating the *M. capensis* exoskeleton; (2) patches of three-dimensional, black multicellular papillate trichomes at variable locations eliciting copulation responses from males landing on the spots; (3) cessation of petal spot development in all but one to four nonadjacent ray florets, turning nectar-guiding rings into isolated spots imitating resting *M. capensis*.[33,34] While all morphotypes produce green-black spot pigment, spots of highly deceptive morphotypes are always both papillate and isolated, non-deceptive morphotypes always possess non-papillate (flat) ring spots, and spots of intermediate forms always lack either papillae or spot isolation.[34] We show that the rapid evolution of sexual deception in *G. diffusa* was propelled by independent co-options of genetic elements affecting the pigmentation, cellular structure, and spatial organization of pre-existing petal spots.

RESULTS

To characterize the molecular basis of sexually deceptive *G. diffusa* petal spots, we first performed mRNA-seq of (1) early developing spotted ray florets of 2–3-mm length from 12 individuals of a highly deceptive morphotype (*G. diffusa* "Springbok"); (2) early developing unspotted florets from the same 12 Springbok individuals; and (3) early developing spotted florets from 12 individuals of a non-deceptive morphotype (*G. diffusa* "Naries"). We *de novo* assembled the Illumina NovaSeq 6000 reads of one individual per morphotype into a combined reference transcriptome, containing a total of 256,858 transcripts with an N_{50} length of 1,386 bp and 90.8% gene completeness. Differential expression (DE) analysis between spotted and unspotted Springbok florets yielded a set of 526 transcripts with a potential role in petal spot formation (Figure 1C). A gene ontology (GO) overrepresentation test identified 15 top-level overrepresented GO terms, 11 of which enriched more than 5-fold (Table S1). To further distinguish general petal spot genes from genes underlying sexually deceptive petal spot components, we conducted a second DE analysis between spotted florets of Springbok and Naries (Figure S2). Intersection of the resulting transcript lists from both DE analyses yielded a subset of 149 transcripts associated with differences in petal spot phenotype between the two morphotypes (triangles in Figure 1C).

Co-option of iron homeostasis genes is associated with altered petal spot pigmentation

Several transcripts DE between spotted and unspotted florets derive from genes of the flavonoid/anthocyanin pigment biosynthesis network (Figures 1C and 2A), including the pathway genes *CHALCONE SYNTHASE* (*GdCHS*), *DIHYDROFLAVONOL 4-REDUCTASE* (*GdDFR*), *ANTHOCYANIDIN SYNTHASE* (*GdANS*), *UDP-GLYCOSLYTRANSFERASE* (*GdUGT*), and *ANTHOCYANIN 3-O-GLUCOSIDE-6″-O-MALONYLTRANSFERASE* (*Gd3MAT*). In addition, the TFs *GdbHLH, GdMYB7*, and *GdMYBSG6* are homologous to characterized TFs from other species, which form the anthocyanin-regulating MYB-bHLH-WD40 TF complexes[35] and match the GO term "regulation of flavonoid biosynthetic process." These results are in line with the findings of Fattorini et al. who showed that the expression of several petal spot-specific *GdMYBSG6* gene copies leads to an accumulation of two red-purple pigments, cyanidin 3-glucoside and a malonylated cyanidin, in the vacuoles of papillae and surrounding epidermal cells of *G. diffusa* Springbok petal spots.[36] Epidermal peels showed that the papillae are indeed dark red, but the surrounding cells show different colors ranging from dark purple to violet and blue, suggesting the presence of other factors influencing coloration (Figure 2B).

Studies in other plant species have shown that complexation of cyanidins with iron shifts their hue from red to blue.[37,38] In *G. diffusa* Springbok, multiple transcripts homologous to iron homeostasis genes in *Arabidopsis thaliana* are differentially expressed in spotted ray florets (Figures 1C and 2A), matching the GO terms "intracellular sequestering of iron ion" and "iron ion transport." Upregulated genes include the *OBP3-RESPONSIVE GENEs ORG1* and *ORG2*, which are strongly induced by iron deficiency in *A. thaliana* leaves and roots.[39] ORG1 (or FIBRILLIN11) is a plastid-localized kinase but its role in iron homeostasis is not understood. ORG2 (bHLH038) induces the expression of many iron uptake genes, including *FERRIC REDUCTION OXIDASE 2* (*FRO2*). FRO2 reduces insoluble ferric ion (Fe^{3+}) chelates to soluble ferrous ions (Fe^{2+}) by transferring electrons across the membrane, enabling the uptake of extracellular iron into the cell by the divalent metal transporter IRT1,[40] although no *G. diffusa* homologs of the latter are found to be upregulated in spotted florets. On the other hand, the gene *OLIGOPEPTIDE TRANSPORTER 3* (*OPT3*) is upregulated, encoding an *OPT* with a specific function in iron transport from the xylem to the phloem.[41] Finally, genes for *NRAMP3/4* and *VACUOLAR IRON TRANSPORTER 1* (*VIT1*), encoding transporters that respectively export iron from and import iron into the vacuole,[42] are upregulated in spotted florets. By contrast, a *FERRITIN* (*FER*) gene is strongly downregulated in spotted florets, indicating that iron is mobilized out of ferritin iron stores.[43] Studies in tulip (*Tulipa gesneriana*) have demonstrated that simultaneous downregulation of *FER* and upregulation of *VIT* not only turns purple anthocyanin-rich petal cells blue but also leads to significant darkening of the blue color.[44–46]

To better understand the expression pattern of the iron homeostasis genes, we quantified the amount of iron by inductively coupled plasma-optical emission spectrometry (ICP-OES) in (1) mature spotted florets, (2) mature unspotted florets, (3) the spotless tip, and (4) the spot-containing base of spotted florets. Zinc and manganese were also measured for comparison and because their metal ions partially share transport mechanisms with iron. Results showed that concentrations of all three elements do not differ significantly between entire spotted and unspotted florets. However, iron concentration is significantly higher in the base, and significantly lower in the tip of spotted florets than the average concentration in entire florets, resulting in a steep 6.9-fold gradient. Zinc also accumulates in the spotted base, but with a much lower 1.3-fold gradient, and manganese is evenly distributed across all tissues (Figure 2C; Table S2). High iron concentration at the base of spotted florets was confirmed with Perls' staining that gives a blue reaction with Fe^{3+} (Figure 2D). Cross sections of the base of spotted florets and enhanced Perls'-diamino benzidine staining, colored dark brown, showed that iron is localized specifically in the papillae

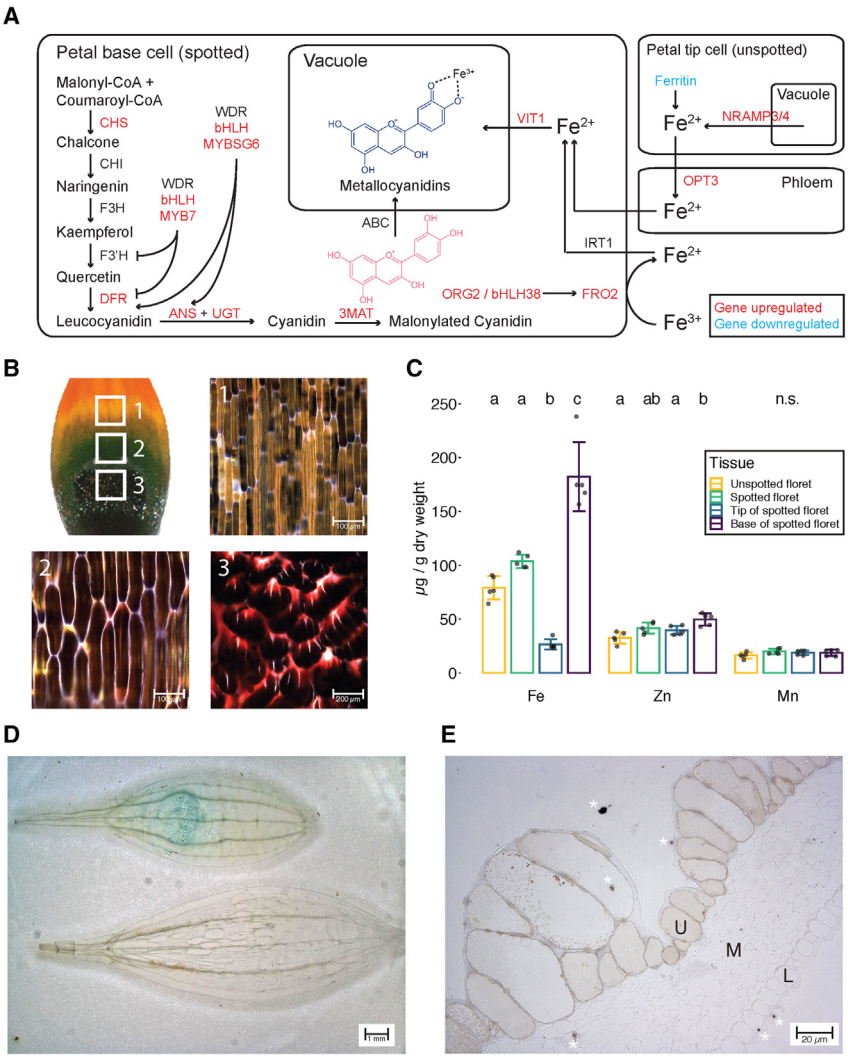

Figure 2. Co-option of iron homeostasis genes is associated with petal spot pigmentation

(A) Simplified diagram of pigment production in *G. diffusa* Springbok petal base spot cells. Two red-purple anthocyanin pigments, cyanidin 3-glucoside and a malonylated cyanidin, are exported into the vacuole where they spontaneously chelate with iron ions imported from petal tip cells, shifting their hue from red to blue.

(B) Light microscopy images of epidermal peels from different areas of a *G. diffusa* Springbok petal spot. The dense cyanidin pigment is violet-blue in small flat petal spot cells (images 1 and 2), but red in the large papillae (image 3). The orange background pigments are carotenoids.

(C) Fe concentration is not different between entire spotted and unspotted Springbok florets but elevated in the base and decreased in tips of spotted florets. Mn concentration does not differ between florets, but Zn concentration follows a similar pattern as it partially shares transport mechanisms with Fe (ANOVA and Tukey HSD post hoc test bars denote mean ± 1 SD, letters denote significant differences among groups, see also Table S2).

(D) Perls' staining detects high quantities of iron in the petal spot area, but not in the surrounding non-spotted tissue of spotted Springbok florets (top, green-blue dye). Unspotted florets show no signal (bottom).

(E) Perls'-DAB staining of quetol-embedded 1-micron slices of spotted florets confirms the presence of iron in the vacuoles of papillae and surrounding upper (adaxial) epidermal cells (brown dye in cell layer labeled U, M denotes mesophyll cell layers, L denotes lower (abaxial) epidermis, and white asterisks denote non-specific dye precipitate).

and surrounding upper (adaxial) epidermal cells, and not in the mesophyll and lower epidermal cell layer, of which only the faint outlines of cell walls are visible (Figure 2E). In agreement with the expectation that iron is in the vacuole, both a disperse brown stain as well as granular aggregates can be seen in this compartment.

Altogether, these results suggest that selected iron homeostasis genes were co-opted to actively accumulate iron in the vacuoles of basal petal spot cells where complexation of iron with cyanidins alters their hue from bright red toward dark blue. Color changes are subtler in the large papillae probably due to the high cyanidin density, but very pronounced in the smaller surrounding epidermal cells. The overlay of violet-blue anthocyanins and yellow-orange carotenoids ultimately results in the perception of the green-black tint within the petal spot area.

Co-option of the root hair gene *GdEXPA7* is associated with the formation of petal spot papillae

G. diffusa petal spots vary not only in coloration but also in shape and positioning of multicellular tongue-like papillate trichomes. Papillae are always present in highly deceptive morphotypes, but completely absent in non-deceptive morphotypes, and form by expansion of adjacent, anthocyanin-filled epidermal cells.[33,34] Of all transcripts DE between spotted and unspotted Springbok florets, the one with the fourth-highest statistical support derives from *GdEXPA7*, a member of the α-*EXPANSIN* gene family (Figure 1C). EXPA proteins relax cell walls via local dissociation of glycans, which leads to irreversible cell expansion,[47] matching the GO term "plant-type cell wall loosening." *GdEXPA7* expression is high in papillate spotted Springbok florets, but close to zero in non-papillate unspotted Springbok florets and spotted Naries florets (Figure 3A). This suggests that *GdEXPA7* is involved in papillae development. In *A. thaliana*, the *EXPA* gene family has 26 members, which differ strongly in their expression pattern, show high tissue specificity, and often have specific roles in individual developmental processes.[48] To further characterize the role of *GdEXPA7*, we reconstructed the phylogenetic relationship of *GdEXPA7* to other *EXPA* copies from *A. thaliana* and sunflower (*Helianthus annuus*). Surprisingly, this analysis placed *GdEXPA7* in a clade consisting of *HaEXPA7*, *AtEXPA7*, and *AtEXPA18* (Figure 3B). In *A. thaliana*, both *AtEXPA7* and *AtEXPA18* are involved in root hair elongation, and thus specifically expressed in developing root hair cells,[49,50] suggesting that *GdEXPA7* is of root origin.

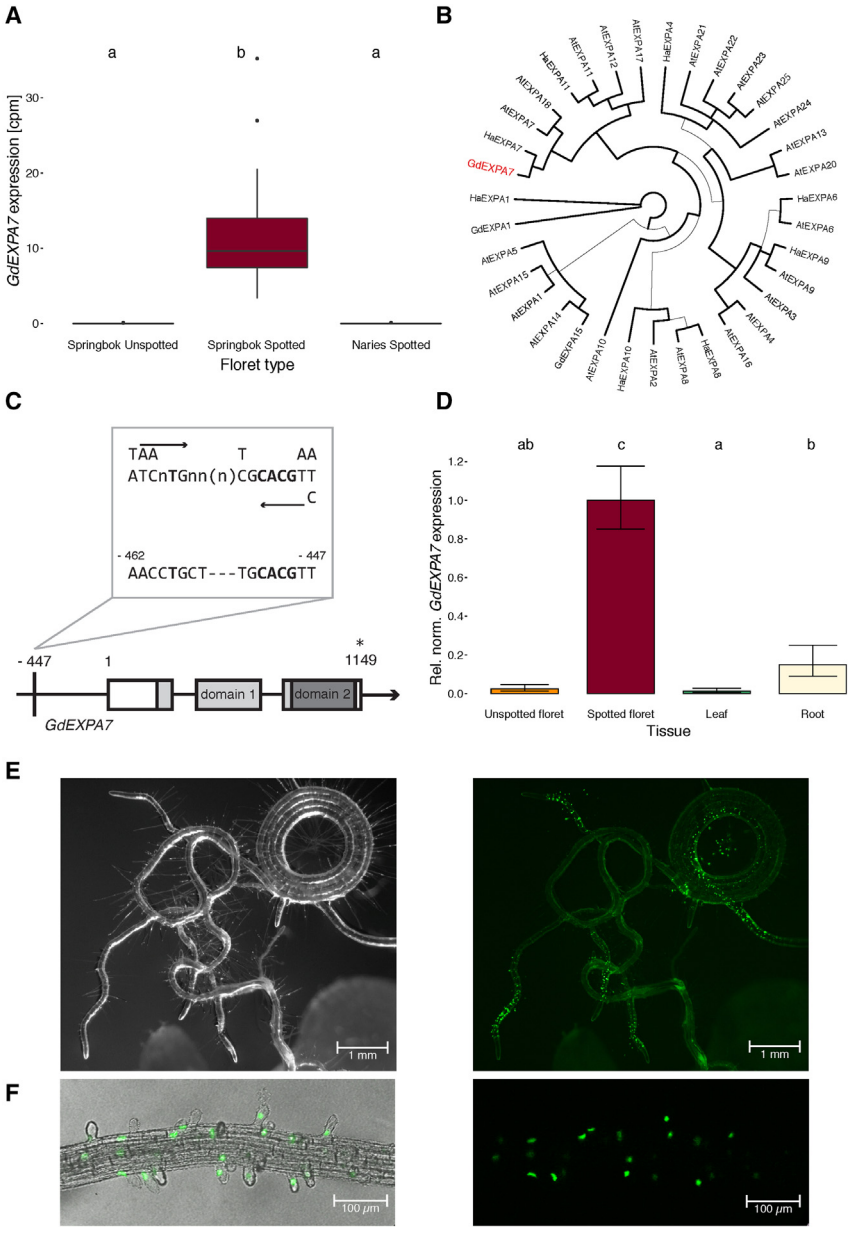

Figure 3. Co-option of the root hair gene *GdEXPA7* is associated with the formation of petal spot papillae

(A) *GdEXPA7* expression is high in papillate spotted Springbok florets, but close to zero in non-papillate unspotted Springbok and spotted Naries florets (quasi-likelihood F test; center lines denote medians, bounds of boxes denote first and third quartiles, whiskers denote 1.5 × interquartile ranges, letters denote significant differences among groups).

(B) Phylogenetic analysis of protein sequences from *A. thaliana* and *H. annuus* EXPA conserved domains 1 and 2 places *GdEXPA7* within the clade of root-specific *EXPA7* and *EXPA18* (bold branches denote posterior probability ≥80%).

(C) *GdEXPA7* contains a root-hair-specific *cis*-regulatory element (RHE) in the promoter region (conserved nucleotides in bold, alternative nucleotides above/below the RHE motif sequence, arrows indicate near-palindromic regions).

(D) RT-qPCR shows that *GdEXPA7* is expressed strongly in developing roots and spotted florets, but not in developing leaves and unspotted florets (ANOVA and Tukey HSD post hoc test, see also Figure S3 and Table S3, bars denote mean ± 1 SEM, letters denote significant differences among groups).

(E) Expression of nuclear localized *GREEN FLUORESCENT PROTEIN* (*GFP-N7*) under the *GdEXPA7* promoter in *A. thaliana* seedlings shows that *GdEXPA7* is active in developing roots (stereo microscopy images with full spectrum illumination).

(F) Close up of developing roots from *GdEXPA7-GFP-N7* transformed *A. thaliana* plants shows that *GdEXPA7* is expressed in developing root hair cells (confocal microscopy images with full spectrum illumination).

A characteristic of *EXPA* genes involved in root hair morphogenesis is the presence of a root-hair-specific *cis*-regulatory element (RHE) in the promoter region. This RHE contains an imperfectly palindromic sequence and is functionally conserved across angiosperms despite divergence of the upstream regulatory cascades.[51] A genome walking approach showed that the promoter sequence of *GdEXPA7* contains a RHE situated 447-bp upstream of the start codon, supporting the hypothesis that *GdEXPA7* is a root hair gene (Figure 3C). To confirm the root hair origin of *GdEXPA7*, we first used RT-qPCR to quantify the expression of *GdEXPA7* in developing roots, leaves, spotted florets, and unspotted florets of *G. diffusa* Springbok. Results showed that *GdEXPA7* expression is close to zero in developing leaves and unspotted florets, moderate in developing roots, and high in developing spotted florets (Figures 3D and S3; Table S3).

Sanger sequencing confirmed that *GdEXPA7* transcripts from root and ray floret cDNA are identical. In a second step, we assessed the activity of the *GdEXPA7* promoter in different *A. thaliana* organs. We transformed *A. thaliana* with a loop assembly plasmid[52] containing a 773-bp fragment upstream of the *GdEXPA7* start codon connected to a nuclear localized *GREEN FLUORESCENT PROTEIN* (*GFP-N7*). *GFP* expression was observed in nuclei of developing root hair cells of transformed T2 seedlings, confirming that *GdEXPA7* is expressed in root hairs (Figures 3E and 3F).

Studies in *A. thaliana* have shown that root hairs develop in response to both developmental and environmental signals. While developmental signals are processed by the *CAPRICE-GLABRA 3-TRANSPARENT TESTA GLABRA 1* (*CPC-GL3-TTG1*) TF complex and the bHLH TF *ROOT HAIR DEFICIENT 6* (*RHD6*), environmental cues are instead transmitted via the phytohormones auxin, abscisic acid, and ethylene.[53] However, none of the genes in these cascades seem to be upregulated in spotted *G. diffusa* florets. Also, while root hairs are single-cell extrusions, the papillae are formed by elongation of multiple

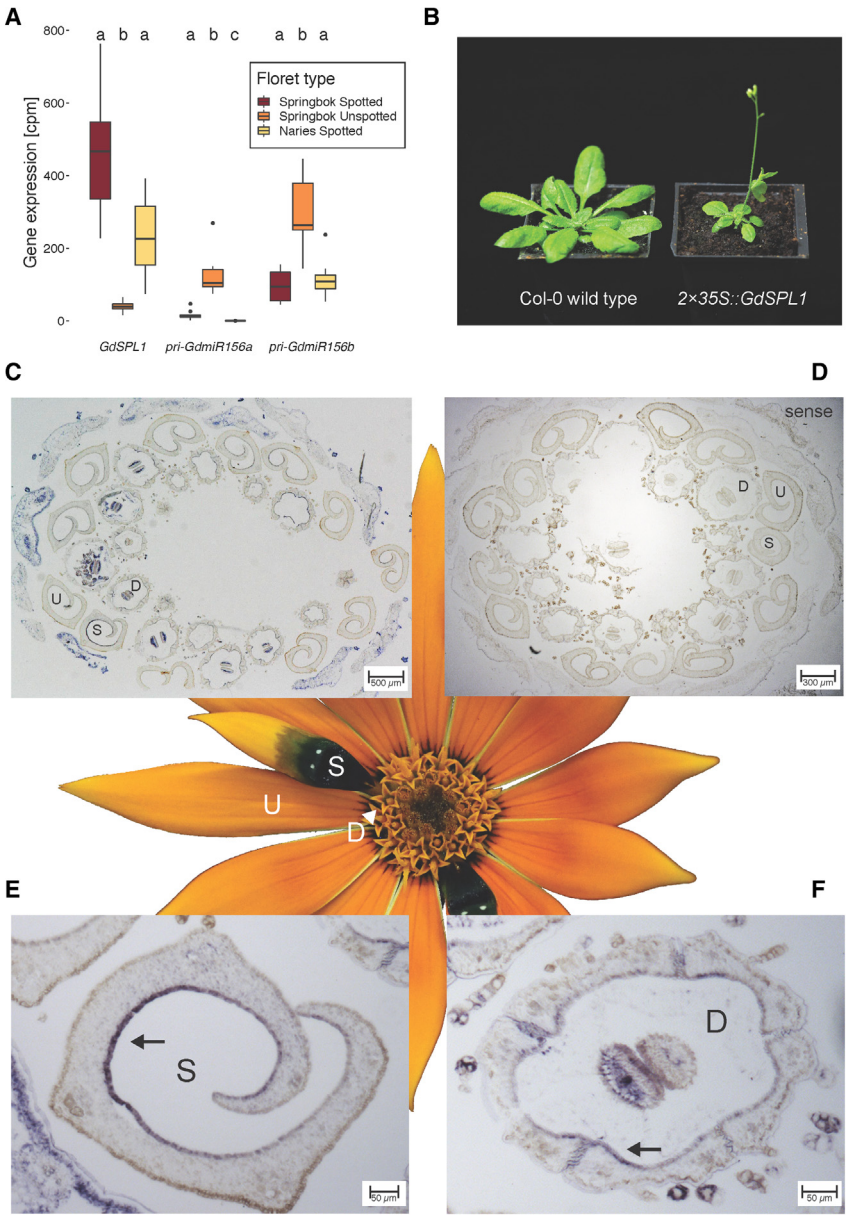

Figure 4. The *GdSPL1* transcription factor is silenced in unspotted ray florets

(A) *GdSPL1* expression is strong in spotted florets of both *G. diffusa* Springbok and Naries, but very weak in unspotted Springbok florets. Expression patterns of the *GdmiR156* precursors *pri-GdmiR156a* and *pri-GdmiR156b* are inverse to *GdSPL1* (quasi-likelihood F test; center lines denote medians, bounds of boxes denote first and third quartiles, whiskers denote 1.5 × interquartile ranges, letters denote significant differences among groups).

(B) Overexpression of *GdSPL1* under a double *35S* promoter induces early flowering in *A. thaliana* (see also Figure S4).

(C) Transverse section of a *G.diffusa* Springbok capitulum hybridized with antisense *GdSPL1* probe; *GdSPL1* is strongly expressed in the petal spot tissue of spotted ray florets (S), but only weakly in unspotted ray florets (U). *GdSPL1* expression is further recorded in the corolla and reproductive organs of disc florets (D).

(D) Transverse section of a *G.diffusa* Springbok capitulum hybridized with sense *GdSPL1* probe (negative control) shows no signal.

(E) Close up of a spotted ray floret hybridized with antisense *GdSPL1* probe; *GdSPL1* is expressed in the epidermis of the ligule (arrow), which consists of fused petals.

(F) Close up of a disc floret hybridized with antisense *GdSPL1* probe; *GdSPL1* expression in the corolla (arrow), which also consists of fused petals, is positionally homologous to spotted ray florets (see also Figure S5).

neighboring cells, suggesting the presence of different regulatory mechanisms. The only other top DE transcript with an obvious connection to root development derives from a gene similar to *ROOT SYSTEM INDUCIBLE 1* (*RSI1*) (Figure 1C).[54] Auxin-induced *RSI1* is expressed during initiation of lateral root growth, but there is no evidence that *GdRSI1* is connected to root hair development or *GdEXPA7* expression. In summary, these results suggest that the root hair gene *GdEXPA7* was co-opted and embedded in the papillae gene network without the upstream root hair signaling cascades.

Co-option of the *GdmiR156-GdSPL1* phase transition module is associated with the spatial rearrangement of petal spots

Besides pigmentation and texture, spatial organization of petal spots on the *G. diffusa* capitulum plays an important role in sexual deception.[34] Ray florets in *G. diffusa* mature basipetally, i.e., the first and oldest ray floret is closest to the center of the capitulum, and successive florets are spaced apart in a golden angle phyllotactic pattern.[33] In the highly deceptive Springbok morphotype, petal spots develop only on the oldest one to four successive ray florets ca. 132° apart (Table S4), breaking up the ring-shaped nectar guide into individual dots resembling flies resting on the capitulum. Based on these observations, Thomas et al. proposed that the signal initiating petal spot development must be turned on in the first ray floret, but then slowly absorbed until it dissipates after one to four florets.[33] Among all transcripts DE between spotted and unspotted *G. diffusa* Springbok florets, the one with the third-highest statistical support derives from a *SQUAMOSA PROMOTER BINDING PROTEIN-LIKE* (*GdSPL1*) gene (Figure 1C). *GdSPL1* is strongly expressed in spotted florets of both the Springbok and Naries morphotype, but very weakly expressed in unspotted Springbok florets (Figure 4A). Since the *SPL* TF family plays an important role in temporal coordination of various processes including phase transitioning and developmental staging,[55] *GdSPL1* could play a role in timing of petal spot development.

To determine its primary function, we expressed *GdSPL1* under a double *35S* promoter in *A. thaliana*. Plants overexpressing

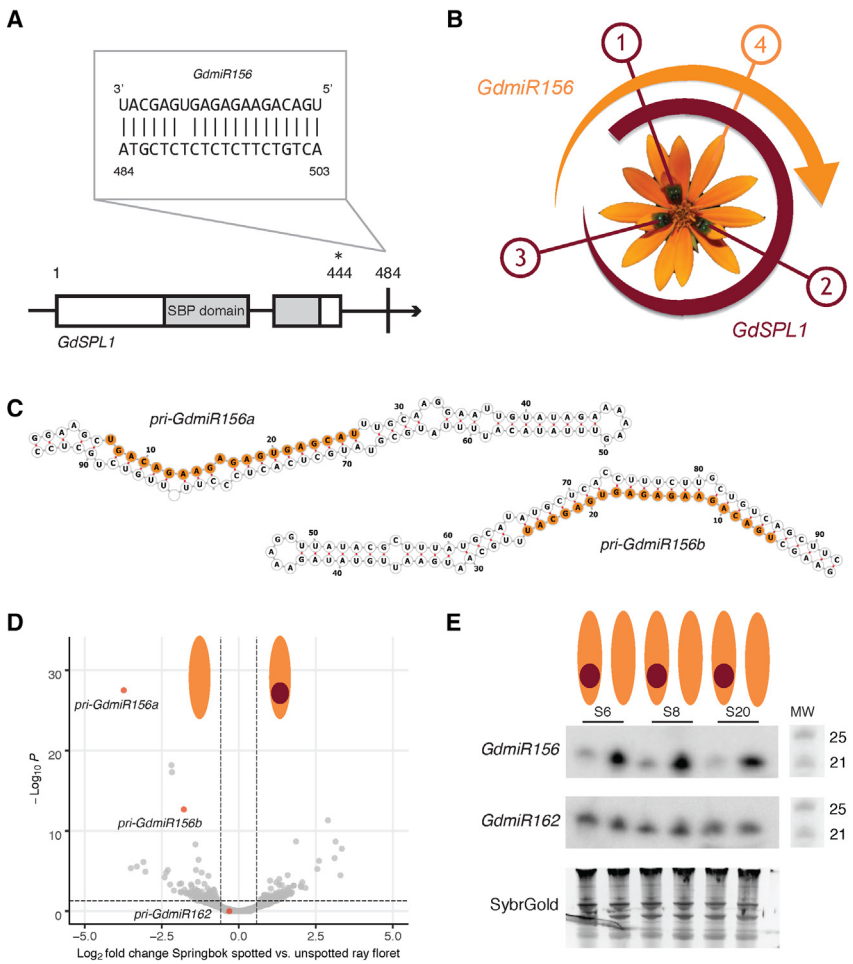

Figure 5. Co-option of the *GdmiR156-GdSPL1* module is associated with petal spot rearrangement

(A) *GdSPL1* contains a *miR156*-binding site 40-bp downstream of the stop codon, which is near-complementary to the *GdmiR156* sequence. Single mismatches are common in plant miRNA-target gene duplexes.

(B) Model of petal spot initiation in *G. diffusa* Springbok. Ray florets develop successively at an angle of ca. 132°. The first few (in this flower: three) ray florets develop under *GdSPL1* expression, which initiates petal spot formation. In subsequently developing ray florets, *GdmiR156* represses *GdSPL1*, terminating the spot developmental program (see also Table S4).

(C) Both *pri-GdmiR156a* and *pri-GdmiR156b* fold to stem-loop hairpin structures typical for microRNA precursors, producing the same mature *GdmiR156*.

(D) Differential expression analysis of small RNAs from spotted and unspotted Springbok ray florets mapped to the *G. diffusa* reference transcriptome (|fold change| ≥ 1.5 and FDR-adjusted p value < 0.05, quasi-likelihood F test). The *pri-GdmiR156a* and *pri-GdmiR156b* precursor transcripts have the highest and fourth-highest statistical support, respectively.

(E) Northern blotting shows that *GdmiR156* expression is high in unspotted florets, but low in spotted Springbok florets. MW denotes an RNA ladder showing single stranded RNA bands of 25 and 21 nt for sizing. *GdmiR162*, a not differentially expressed miRNA, serves as control for transfer and equal loading (see D), and SybrGold staining of total RNA as loading control (S6, S8, and S20 denote *G. diffusa* individuals).

GdSPL1 flowered at an earlier time point than wild-type *A. thaliana* plants, suggesting that *GdSPL1* is involved in vegetative to generative phase transitioning and flower initiation (Figures 4B and S4). Phase transitioning *SPL* have been shown to negatively regulate some anthocyanin MBW TF complexes in vegetative tissue of other plant species.[56,57] However, *in situ* hybridization of the *GdSPL1* transcript in developing *G. diffusa* Springbok buds showed that *GdSPL1* is expressed in the anthocyanin-rich petal spot area (adaxial epidermis of the tongue-shaped ligule of spotted ray florets, Figures 4C–4E), suggesting no negative interaction between GdSPL1 and GdMYBSG6. *GdSPL1* is also expressed in the adaxial epidermis of disc floret corollas (Figures 4C–4F). Since both the ligule of ray florets and the corolla of disc florets consist of fused petals, *GdSPL1* expression is positionally homologous in both floret types. As expected, *GdSPL1* expression was very weak in unspotted ray florets. *In situ* hybridization of the same *GdSPL1* probe in developing *G. diffusa* Naries buds further showed a signal in all ray florets, as expected in morphotypes with ring spots (Figure S5). In summary, this suggests that the *GdSPL1* signal is present in all petals from an early time point in capitulum development up to the maturation of spotted florets and is then actively repressed in later developing unspotted florets of the Springbok morphotype. Studies have shown that a subset of *SPL* genes is post-transcriptionally regulated in a quantitative fashion by microRNAs from the *miR156* family via cleavage or translational repression of *SPL* transcripts.[55,58] A closer inspection of the *GdSPL1* transcript confirmed the presence of a *miR156*-binding site in the 3′ UTR (Figure 5A). Downregulation of *GdSPL1* in unspotted *G. diffusa* florets could therefore be small RNA mediated (Figure 5B).

To test this hypothesis, we first searched the *G. diffusa* reference transcriptome for differentially expressed primary *miR156* precursors complementary to the *miR156* binding site in *GdSPL1*. The transcripts *pri-GdmiR156a* and *pri-GdmiR156b* both contain the same near-complementary miR156 sequence (one mismatch, Figure 5A), and *in-silico* predictions showed that they both fold to a stem-loop structure as known from miRNA precursors (Figure 5C). Mismatches are common in plant miRNA-target gene duplexes, especially in the miRNA 3′ regions, and can sometimes even enhance the silencing efficiency.[59] The expression level of both precursor transcripts is significantly higher in unspotted Springbok florets than in spotted Springbok and spotted Naries florets (Figures 1C and 4A). To assess the expression of mature miRNAs in Springbok, we performed small RNA-seq of spotted and unspotted ray florets from four individuals using the same tissue as for the mRNA-seq analysis. We mapped all reads to (1) the combined mRNA reference assembly

and (2) all mature miRNAs from the miRbase database[60] and conducted a DE analysis with each. Among the transcripts with the highest statistical support are the two *pri-GdmiR156* precursors from the mRNA reference assembly (Figure 5D), and the mature miRNAs *AmamiR156, stu-miR156f-5p*, and *cca-miR156b* from miRbase, respectively. Northern blotting of the same small RNA extractions confirmed that *GdmiR156* expression is high in unspotted florets, but low in spotted florets of Springbok (Figure 5E). Overall, these results suggest that the *GdmiR156-GdSPL1* phase transition module was co-opted to provide the spatiotemporal information required for the initiation and cessation of petal spot development in *G. diffusa* Springbok.

DISCUSSION

Within the last decades, gene co-option has emerged as a major mechanism underlying the rapid appearance of evolutionary novelties.[2,61] The cases investigated to date exemplify the action of co-option on multiple levels, from single gene recruitment[62] to partial network co-option[4] and co-option of entire gene cascades.[7] Nevertheless, their evolutionary trajectory is rarely determinable due to the derived nature of such traits. In contrast, the existence of intermediately deceptive *G. diffusa* morphotypes allows partitioning of the complex deceptive petal spot phenotype into its individually evolved components. We not only detected a co-option event in the evolutionary history of each component, but also these events span from single gene recruitment to co-option of a partial gene network and include both structural and regulatory modules. Unlike most other documented cases, the *G. diffusa* petal spots are thus not an evolutionary consequence of a single, major gene network co-option but rather represent a modular integration of multiple independent and highly diverse co-option events. Puzzling composite novelties have been described in a wide range of organisms,[63–65] suggesting that such modular co-options are relatively common. However, their relative importance in comparison with other evolutionary mechanisms such as gene duplication remains to be determined.

Plant sexual deception has fascinated biologists for centuries,[66] but the evolution of sexually deceptive flowers remains somewhat enigmatic due to their extreme specialization and the absence of intermediately deceptive forms. The recently resolved phylogenetic tree of *G. diffusa* morphotypes[29] suggests that the sexually deceptive petal spot components evolved sequentially with spot pigmentation emerging first (before the origin of *G. diffusa*), followed by spot rearrangement and the production of papillae, eventually resulting in the evolution of highly deceptive morphotypes in two independent clades. This pattern suggests that the co-option events studied here likely also occurred sequentially through the evolution of the group and raises questions about the selective pressures favoring each event. A likely scenario, which needs further experimental testing, is that the initial changes to spot pigmentation and arrangement increased attention from mate searching male flies,[32] which are better pollinators than less mobile females,[28] while the later development of papillae elicited physical interaction between male flies and petal spots (i.e., pseudocopulation),[32] allowing direct exploitation of mating flies for pollination.

Strong selective pressure imposed by mating male pollinators usually results in tight integration of the various visual, haptic, and olfactory components of sexually deceptive flowers. While all *G. diffusa* morphotypes show considerable phenotypic variation in petal spot morphology (particularly spot dimensions), Ellis et al. found that the integration of floral traits involved in visual attraction of *M. capensis* males is indeed elevated in highly deceptive morphotypes. In this case, male pollinators do not select for absolute dimensions and positions of petal spot components but rather strengthen the developmental integration of different trait combinations eliciting sexual deception.[34] Evolution of sexual deception in *G. diffusa* was thus likely a two-step process with a first phase of rapid, excessive tinkering with independently co-opted genetic modules followed by a phase of pollinator-mediated integration of the most deceptive module combinations.

Our study indicates several directions for further investigations of the underlying evolutionary-developmental processes. First, tissue-specific gene expression and protein interaction studies may uncover more elements of the genetic pathways underlying petal spot formation. Second, transgenic manipulation of *G. diffusa* may allow functional verification of the co-opted genetic elements. Third, genomic comparisons among morphotypes and their hybrids may further elucidate the evolutionary trajectory of plant sexual deception. Altogether, these analyses may contribute to a better understanding of gene co-option in general, including its genetic initiation, fine-tuning, and possible pleiotropic effects.

In conclusion, our study shows that a modular integration of multiple independently co-opted genetic elements can facilitate the evolution of complex phenotypic novelties.

STAR★METHODS

Detailed methods are provided in the online version of this paper and include the following:

- KEY RESOURCES TABLE
- RESOURCE AVAILABILITY
  - Lead contact
  - Materials availability
  - Data and code availability
- EXPERIMENTAL MODEL AND SUBJECT DETAILS
  - Gorteria diffusa cultivation
  - *Arabidopsis thaliana* cultivation
- METHOD DETAILS
  - Transcriptome assembly and annotation
  - Gene expression and overrepresentation test
  - CryoSEM imaging
  - ICP-OES
  - Perls'-DAB staining and microscopy
  - Phylogenetic analysis of *GdEXPA7*
  - Analysis of *GdEXPA7* promoter sequence
  - RT-qPCR of *GdEXPA7* in *G. diffusa* tissues
  - Cloning of *GdEXPA7* promoter reporter plasmid
  - Localisation of *GdEXPA7* promoter activity
  - Angle measurements of *G. diffusa* ray florets
  - *GdSPL1* expression in *A. thaliana*
  - *In-situ* hybridisation of *GdSPL1*

- Detection and folding of *pri-GdmiR156*
- Differential expression analysis of small RNA
- Northern blotting of *GdmiR156* and *GdmiR162*

● QUANTIFICATION AND STATISTICAL ANALYSIS

SUPPLEMENTAL INFORMATION

Supplemental information can be found online at https://doi.org/10.1016/j.cub.2023.03.003.

ACKNOWLEDGMENTS

We thank Matthew Dorling and Emma Jackson for plant rearing and technical support, and Dr. Eftychios Frangedakis, Dr. Chiara Airoldi, Dr. James Connorton, Rose McNelly, Dr. Weibing Yang, Dr. Raymond Wightman, and Dr. Hamish Symington for assistance and material for lab experiments. We also thank Prof. Daniel Cosgrove, Prof. Ottoline Leyser, Prof. Philipp Schlüter, Dr. Elinor Jax, and Farahnoz Khojayori for helpful discussions, and three anonymous reviewers for constructive feedback. We further thank the Northern Cape Department of Environment and Nature Conservation for issuing a collection permit (FLORA 0057/2018). This study was funded by a Swiss National Science Foundation (SNSF) Early Postdoc.Mobility grant to R.T.K. (fellowship P2ZHP3_178043), an Isaac Newton Trust grant to R.T.K. and B.J.G., a Natural Environment Research Council (NERC) grant to B.J.G. and A.G.E. (NE/P011764/1), and a Biotechnology and Biological Sciences Research Council (BBSRC) grant to B.J.G. (BB/V000314/1). S.L.-G. is a senior Broodbank Research Fellow. The cryoSEM facility at the Sainsbury Laboratory, Cambridge is supported by the Gatsby Charitable Foundation.

AUTHOR CONTRIBUTIONS

R.T.K., B.J.G., A.G.E., and J.B. conceived and designed this study. A.G.E. and B.J.G. collected *G. diffusa* seeds. R.T.K. and R.F. cultivated the *G. diffusa* plants. R.T.K. and B.D. conducted the transcriptome assembly and analysis. J.B. and R.T.K. performed the ICP-OES analysis. K.H.M., U.P., and R.T.K. conducted the iron localization analyses. R.T.K. carried out the phylogenetic analyses, R.T.K. and R.F. conducted the genetic analyses. U.P. did the *in situ* hybridization. R.T.K. and S.L.-G. performed the small RNA analysis. R.T.K. wrote the original draft of the manuscript with inputs from B.J.G., A.G.E., and J.B. All authors discussed and approved the final manuscript. B.J.G., A.G.E., and J.B. provided resources for this study. R.T.K., B.J.G., and A.G.E. acquired funding for this project.

DECLARATION OF INTERESTS

B.J.G. is a member of the advisory board of *Current Biology*.

Received: January 5, 2023
Revised: February 28, 2023
Accepted: March 1, 2023
Published: March 23, 2023

REFERENCES

1. True, J.R., and Carroll, S.B. (2002). Gene co-option in physiological and morphological evolution. Annu. Rev. Cell Dev. Biol. *18*, 53–80.
2. McQueen, E., and Rebeiz, M. (2020). On the specificity of gene regulatory networks: how does network co-option affect subsequent evolution? Curr. Top. Dev. Biol. *139*, 375–405.
3. Monteiro, A., and Podlaha, O. (2009). Wings, horns, and butterfly eyespots: how do complex traits evolve? PLoS Biol. *7*, e37.
4. Hu, Y., Schmitt-Engel, C., Schwirz, J., Stroehlein, N., Richter, T., Majumdar, U., and Bucher, G. (2018). A morphological novelty evolved by co-option of a reduced gene regulatory network and gene recruitment in a beetle. Proc. Biol. Sci. *285*, 20181373.
5. Aguilera, F., McDougall, C., and Degnan, B.M. (2017). Co-option and de novo gene evolution underlie molluscan shell diversity. Mol. Biol. Evol. *34*, 779–792.
6. Hilgers, L., Hartmann, S., Hofreiter, M., and von Rintelen, T. (2018). Novel genes, ancient genes, and gene co-option contributed to the genetic basis of the radula, a molluscan innovation. Mol. Biol. Evol. *35*, 1638–1652.
7. Tomoyasu, Y., Arakane, Y., Kramer, K.J., and Denell, R.E. (2009). Repeated co-options of exoskeleton formation during wing-to-elytron evolution in beetles. Curr. Biol. *19*, 2057–2065.
8. Özsu, N., and Monteiro, A. (2017). Wound healing, calcium signaling, and other novel pathways are associated with the formation of butterfly eyespots. BMC Genomics *18*, 788.
9. de Almeida, A.M.R., Yockteng, R., Schnable, J., Alvarez-Buylla, E.R., Freeling, M., and Specht, C.D. (2014). Co-option of the polarity gene network shapes filament morphology in angiosperms. Sci. Rep. *4*, 6194.
10. Schiestl, F.P., Ayasse, M., Paulus, H.F., Löfstedt, C., Hansson, B.S., Ibarra, F., and Francke, W. (1999). Orchid pollination by sexual swindle. Nature *399*, 421.
11. Bohman, B., Flematti, G.R., Barrow, R.A., Pichersky, E., and Peakall, R. (2016). Pollination by sexual deception—it takes chemistry to work. Curr. Opin. Plant Biol. *32*, 37–46.
12. de Jager, M.L., and Peakall, R. (2016). Does morphology matter? An explicit assessment of floral morphology in sexual deception. Funct. Ecol. *30*, 537–546.
13. Ågren, L., Kullenberg, B., and Sensenbaugh, T. (1983). Congruences in pilosity between three species of *Ophrys* (Orichidaceae) and their hymenopteran pollinators. Nova Acta Reg. Soc. Sci. Ups. *3*, 15–25.
14. Peakall, R., Ebert, D., Poldy, J., Barrow, R.A., Francke, W., Bower, C.C., and Schiestl, F.P. (2010). Pollinator specificity, floral odour chemistry and the phylogeny of Australian sexually deceptive *Chiloglottis* orchids: implications for pollinator-driven speciation. New Phytol. *188*, 437–450.
15. Reiter, N., Freestone, M., Brown, G., and Peakall, R. (2019). Pollination by sexual deception of fungus gnats (Keroplatidae and Mycetophilidae) in two clades of *Pterostylis* (Orchidaceae). Bot. J. Linn. Soc. *190*, 101–116.
16. Sedeek, K.E., Qi, W., Schauer, M.A., Gupta, A.K., Poveda, L., Xu, S., Liu, Z.J., Grossniklaus, U., Schiestl, F.P., and Schlüter, P.M. (2013). Transcriptome and proteome data reveal candidate genes for pollinator attraction in sexually deceptive orchids. PLoS One *8*, e64621.
17. Vignolini, S., Davey, M.P., Bateman, R.M., Rudall, P.J., Moyroud, E., Tratt, J., Malmgren, S., Steiner, U., and Glover, B.J. (2012). The mirror crack'd: both pigment and structure contribute to the glossy blue appearance of the mirror orchid, Ophrys speculum. New Phytol. *196*, 1038–1047.
18. Wong, D.C.J., Amarasinghe, R., Falara, V., Pichersky, E., and Peakall, R. (2019). Duplication and selection in *β-ketoacyl-ACP synthase* gene lineages in the sexually deceptive *Chiloglottis* (Orchidaceace). Ann. Bot. *123*, 1053–1066.
19. Xu, H., Bohman, B., Wong, D.C.J., Rodriguez-Delgado, C., Scaffidi, A., Flematti, G.R., Phillips, R.D., Pichersky, E., and Peakall, R. (2017). Complex sexual deception in an orchid is achieved by co-opting two independent biosynthetic pathways for pollinator attraction. Curr. Biol. *27*, 1867–1877.e5.
20. Sedeek, K.E., Whittle, E., Guthörl, D., Grossniklaus, U., Shanklin, J., and Schlüter, P.M. (2016). Amino acid change in an orchid desaturase enables mimicry of the pollinator's sex pheromone. Curr. Biol. *26*, 1505–1511.
21. Xu, S., and Schlüter, P.M. (2015). Modeling the two-locus architecture of divergent pollinator adaptation: how variation in *SAD* paralogs affects fitness and evolutionary divergence in sexually deceptive orchids. Ecol. Evol. *5*, 493–502.
22. Cohen, C., Liltved, W.R., Colville, J.F., Shuttleworth, A., Weissflog, J., Svatoš, A., Bytebier, B., and Johnson, S.D. (2021). Sexual deception of a beetle pollinator through floral mimicry. Curr. Biol. *31*, 1962–1969.e6.
23. Arakaki, N., Yasuda, K., Kanayama, S., Jitsuno, S., Oike, M., and Wakamura, S. (2016). Attraction of males of the cupreous polished chafer *Protaetia pryeri pryeri* (Coleoptera: Scarabaeidae) for pollination by an

epiphytic orchid *Luisia teres* (Asparagales: Orchidaceae). Appl. Entomol. Zool. *51*, 241–246.

24. Cozzolino, S., and Widmer, A. (2005). Orchid diversity: an evolutionary consequence of deception? Trends Ecol. Evol. *20*, 487–494.
25. Vereecken, N.J., Wilson, C.A., Hötling, S., Schulz, S., Banketov, S.A., and Mardulyn, P. (2012). Pre-adaptations and the evolution of pollination by sexual deception: Cope's rule of specialization revisited. Proc. Biol. Sci. *279*, 4786–4794.
26. Bohman, B., Phillips, R.D., Menz, M.H., Berntsson, B.W., Flematti, G.R., Barrow, R.A., Dixon, K.W., and Peakall, R. (2014). Discovery of pyrazines as pollinator sex pheromones and orchid semiochemicals: implications for the evolution of sexual deception. New Phytol. *203*, 939–952.
27. Johnson, S.D., and Midgley, J.J. (1997). Fly pollination of *Gorteria diffusa* (Asteraceae), and a possible mimetic function for dark spots on the capitulum. Am. J. Bot. *84*, 429.
28. Ellis, A.G., and Johnson, S.D. (2010). Floral mimicry enhances pollen export: the evolution of pollination by sexual deceit outside of the Orchidaceae. Am. Nat. *176*, E143–E151.
29. Delahaie, B., Mellers, G., Kellenberger, R.T., Fernández-Mazuecos, M., Fattorini, R., Brockington, S.F., Ellis, A.G., and Glover, B.J. (2022). The phylogenetic history of the *Gorteria diffusa* radiation sheds light on the origins of plant sexual deception. Preprint at bioRxiv. https://doi.org/10.1101/2022.12.22.521170.
30. Ellis, A.G., and Johnson, S.D. (2009). The evolution of floral variation without pollinator shifts in *Gorteria diffusa* (Asteraceae). Am. J. Bot. *96*, 793–801.
31. de Jager, M.L., Willis-Jones, E., Critchley, S., and Glover, B.J. (2017). The impact of floral spot and ring markings on pollinator foraging dynamics. Evol. Ecol. *31*, 193–204.
32. de Jager, M.L., and Ellis, A.G. (2012). Gender-specific pollinator preference for floral traits. Funct. Ecol. *26*, 1197–1204.
33. Thomas, M.M., Rudall, P.J., Ellis, A.G., Savolainen, V., and Glover, B.J. (2009). Development of a complex floral trait: the pollinator-attracting petal spots of the beetle daisy, *Gorteria diffusa* (Asteraceae). Am. J. Bot. *96*, 2184–2196.
34. Ellis, A.G., Brockington, S.F., de Jager, M.L., Mellers, G., Walker, R.H., and Glover, B.J. (2014). Floral trait variation and integration as a function of sexual deception in *Gorteria diffusa*. Philos. Trans. R. Soc. Lond. B Biol. Sci. *369*, 20130563.
35. Yan, H., Pei, X., Zhang, H., Li, X., Zhang, X., Zhao, M., Chiang, V.L., Sederoff, R.R., and Zhao, X. (2021). MYB-mediated regulation of anthocyanin biosynthesis. Int. J. Mol. Sci. *22*, 3103.
36. Fattorini, R., Khojayori, F., Mellers, G., Moyroud, E., Herrero Serrano, E., Kellenberger, R.T., Walker, R., Wang, Q., Hill, L., and Glover, B.J. (2023). Complex petal spot formation in the Beetle Daisy (*Gorteria diffusa*) relies on spot-specific accumulation of malonylated anthocyanin regulated by paralogous GdMYBSG6 transcription factors. Preprint at bioRxiv. https://doi.org/10.1101/2023.02.20.529304.
37. Yoshida, K., and Negishi, T. (2013). The identification of a vacuolar iron transporter involved in the blue coloration of cornflower petals. Phytochemistry *94*, 60–67.
38. Yoshida, K., Kitahara, S., Ito, D., and Kondo, T. (2006). Ferric ions involved in the flower color development of the Himalayan blue poppy, *Meconopsis grandis*. Phytochemistry *67*, 992–998.
39. Rodríguez-Celma, J., Pan, I.C., Li, W., Lan, P., Buckhout, T.J., and Schmidt, W. (2013). The transcriptional response of *Arabidopsis* leaves to Fe deficiency. Front. Plant Sci. *4*, 276.
40. Robinson, N.J., Procter, C.M., Connolly, E.L., and Guerinot, M.L. (1999). A ferric-chelate reductase for iron uptake from soils. Nature *397*, 694–697.
41. Zhai, Z., Gayomba, S.R., Jung, H.I., Vimalakumari, N.K., Piñeros, M., Craft, E., Rutzke, M.A., Danku, J., Lahner, B., Punshon, T., et al. (2014). OPT3 is a phloem-specific iron transporter that is essential for systemic iron signaling and redistribution of iron and cadmium in *Arabidopsis*. Plant Cell *26*, 2249–2264.
42. Connorton, J.M., Balk, J., and Rodríguez-Celma, J. (2017). Iron homeostasis in plants–a brief overview. Metallomics *9*, 813–823.
43. Ravet, K., Touraine, B., Boucherez, J., Briat, J.F., Gaymard, F., and Cellier, F. (2009). Ferritins control interaction between iron homeostasis and oxidative stress in *Arabidopsis*. Plant J. *57*, 400–412.
44. Momonoi, K., Tsuji, T., Kazuma, K., and Yoshida, K. (2012). Specific expression of the vacuolar iron transporter, *TgVit*, causes iron accumulation in blue-colored inner bottom segments of various tulip petals. Biosci. Biotechnol. Biochem. *76*, 319–325.
45. Momonoi, K., Yoshida, K., Mano, S., Takahashi, H., Nakamori, C., Shoji, K., Nitta, A., and Nishimura, M. (2009). A vacuolar iron transporter in tulip, TgVit1, is responsible for blue coloration in petal cells through iron accumulation. Plant J. *59*, 437–447.
46. Shoji, K., Momonoi, K., and Tsuji, T. (2010). Alternative expression of vacuolar iron transporter and ferritin genes leads to blue/purple coloration of flowers in tulip cv.'Murasakizuisho'. Plant Cell Physiol. *51*, 215–224.
47. Cosgrove, D.J. (2000). Loosening of plant cell walls by expansins. Nature *407*, 321–326.
48. Sampedro, J., and Cosgrove, D.J. (2005). The expansin superfamily. Genome Biol. *6*, 242.
49. Cho, H.-T., and Cosgrove, D.J. (2002). Regulation of root hair initiation and expansin gene expression in *Arabidopsis*. Plant Cell *14*, 3237–3253.
50. Lin, C., Choi, H.-S., and Cho, H.-T. (2011). Root hair-specific EXPANSIN A7 is required for root hair elongation in *Arabidopsis*. Mol. Cells *31*, 393–397.
51. Kim, D.W., Lee, S.H., Choi, S.-B., Won, S.-K., Heo, Y.-K., Cho, M., Park, Y.-I., and Cho, H.-T. (2006). Functional conservation of a root hair cell-specific *cis*-element in angiosperms with different root hair distribution patterns. Plant Cell *18*, 2958–2970.
52. Pollak, B., Cerda, A., Delmans, M., Álamos, S., Moyano, T., West, A., Gutiérrez, R.A., Patron, N.J., Federici, F., and Haseloff, J. (2019). Loop assembly: a simple and open system for recursive fabrication of DNA circuits. New Phytol. *222*, 628–640.
53. Shibata, M., and Sugimoto, K. (2019). A gene regulatory network for root hair development. J. Plant Res. *132*, 301–309.
54. Taylor, B.H., and Scheuring, C.F. (1994). A molecular marker for lateral root initiation: the *RSI-1* gene of tomato (*Lycopersicon esculentum* Mill) is activated in early lateral root primordia. Mol. Gen. Genet. *243*, 148–157.
55. Preston, J.C., and Hileman, L.C. (2013). Functional evolution in the plant *squamosa-PROMOTER BINDING PROTEIN-LIKE* (*SPL*) gene family. Front. Plant Sci. *4*, 80.
56. Gou, J.-Y., Felippes, F.F., Liu, C.-J., Weigel, D., and Wang, J.-W. (2011). Negative regulation of anthocyanin biosynthesis in *Arabidopsis* by a miR156-targeted SPL transcription factor. Plant Cell *23*, 1512–1522.
57. Wang, Y., Liu, W., Wang, X., Yang, R., Wu, Z., Wang, H., Wang, L., Hu, Z., Guo, S., Zhang, H., et al. (2020). MiR156 regulates anthocyanin biosynthesis through *SPL* targets and other microRNAs in poplar. Hortic. Res. *7*, 118.
58. Wang, J.-W., Schwab, R., Czech, B., Mica, E., and Weigel, D. (2008). Dual effects of miR156-targeted *SPL* genes and *CYP78A5/KLUH* on plastochron length and organ size in *Arabidopsis thaliana*. Plant Cell *20*, 1231–1243.
59. Liu, Q., Wang, F., and Axtell, M.J. (2014). Analysis of complementarity requirements for plant microRNA targeting using a *Nicotiana benthamiana* quantitative transient assay. Plant Cell *26*, 741–753.
60. Kozomara, A., Birgaoanu, M., and Griffiths-Jones, S. (2019). miRBase: from microRNA sequences to function. Nucleic Acids Res. *47*, D155–D162.
61. Oakley, T.H. (2017). Furcation and fusion: the phylogenetics of evolutionary novelty. Dev. Biol. *431*, 69–76.
62. Martin, A., McCulloch, K.J., Patel, N.H., Briscoe, A.D., Gilbert, L.E., and Reed, R.D. (2014). Multiple recent co-options of Optix associated with novel traits in adaptive butterfly wing radiations. EvoDevo *5*, 7.

63. Stansbury, M.S., and Moczek, A.P. (2014). The function of *Hox* and appendage-patterning genes in the development of an evolutionary novelty, the *Photuris* firefly lantern. Proc. Biol. Sci. *281*, 20133333.
64. Hedrich, R., and Fukushima, K. (2021). On the origin of carnivory: molecular physiology and evolution of plants on an animal diet. Annu. Rev. Plant Biol. *72*, 133–153.
65. Zancolli, G., and Casewell, N.R. (2020). Venom systems as models for studying the origin and regulation of evolutionary novelties. Mol. Biol. Evol. *37*, 2777–2790.
66. Darwin, C. (1888). The various contrivances by which orchids are fertilised by insects (J. Murray).
67. Hellens, R.P., Edwards, E.A., Leyland, N.R., Bean, S., and Mullineaux, P.M. (2000). pGreen: a versatile and flexible binary Ti vector for *Agrobacterium*-mediated plant transformation. Plant Mol. Biol. *42*, 819–832.
68. Bolger, A.M., Lohse, M., and Usadel, B. (2014). Trimmomatic: a flexible trimmer for Illumina sequence data. Bioinformatics *30*, 2114–2120.
69. Grabherr, M.G., Haas, B.J., Yassour, M., Levin, J.Z., Thompson, D.A., Amit, I., Adiconis, X., Fan, L., Raychowdhury, R., Zeng, Q., et al. (2011). Full-length transcriptome assembly from RNA-Seq data without a reference genome. Nat. Biotechnol. *29*, 644–652.
70. Haas, B.J., Papanicolaou, A., Yassour, M., Grabherr, M., Blood, P.D., Bowden, J., Couger, M.B., Eccles, D., Li, B., Lieber, M., et al. (2013). De novo transcript sequence reconstruction from RNA-seq using the Trinity platform for reference generation and analysis. Nat. Protoc. *8*, 1494–1512.
71. Bryant, D.M., Johnson, K., DiTommaso, T., Tickle, T., Couger, M.B., Payzin-Dogru, D., Lee, T.J., Leigh, N.D., Kuo, T.-H., Davis, F.G., et al. (2017). A tissue-mapped axolotl de novo transcriptome enables identification of limb regeneration factors. Cell Rep. *18*, 762–776.
72. Simão, F.A., Waterhouse, R.M., Ioannidis, P., Kriventseva, E.V., and Zdobnov, E.M. (2015). BUSCO: assessing genome assembly and annotation completeness with single-copy orthologs. Bioinformatics *31*, 3210–3212.
73. Li, B., and Dewey, C.N. (2011). RSEM: accurate transcript quantification from RNA-Seq data with or without a reference genome. BMC Bioinformatics *12*, 323.
74. Langmead, B., and Salzberg, S.L. (2012). Fast gapped-read alignment with Bowtie 2. Nat. Methods *9*, 357–359.
75. R Core Team (2018). R: A language and environment for statistical computing (Vienna, Austria: R Foundation for Statistical Computing).
76. Soneson, C., Love, M.I., and Robinson, M.D. (2015). Differential analyses for RNA-seq: transcript-level estimates improve gene-level inferences. F1000Res. *4*, 1521.
77. Robinson, M.D., McCarthy, D.J., and Smyth, G.K. (2010). edgeR: a Bioconductor package for differential expression analysis of digital gene expression data. Bioinformatics *26*, 139–140.
78. Mi, H., Ebert, D., Muruganujan, A., Mills, C., Albou, L.-P., Mushayamaha, T., and Thomas, P.D. (2021). PANTHER version 16: a revised family classification, tree-based classification tool, enhancer regions and extensive API. Nucleic Acids Res. *49*, D394–D403.
79. Kumar, S., Stecher, G., and Tamura, K. (2016). MEGA7: molecular evolutionary genetics analysis version 7.0 for bigger datasets. Mol. Biol. Evol. *33*, 1870–1874.
80. Darriba, D., Taboada, G.L., Doallo, R., and Posada, D. (2011). ProtTest 3: fast selection of best-fit models of protein evolution. Bioinformatics *27*, 1164–1165.
81. Ronquist, F., Teslenko, M., Van Der Mark, P., Ayres, D.L., Darling, A., Höhna, S., Larget, B., Liu, L., Suchard, M.A., and Huelsenbeck, J.P. (2012). MrBayes 3.2: efficient Bayesian phylogenetic inference and model choice across a large model space. Syst. Biol. *61*, 539–542.
82. Schneider, C.A., Rasband, W.S., and Eliceiri, K.W. (2012). NIH Image to ImageJ: 25 years of image analysis. Nat. Methods *9*, 671–675.
83. Altschul, S.F., Madden, T.L., Schäffer, A.A., Zhang, J., Zhang, Z., Miller, W., and Lipman, D.J. (1997). Gapped BLAST and PSI-BLAST: a new generation of protein database search programs. Nucleic Acids Res. *25*, 3389–3402.
84. Lorenz, R., Bernhart, S.H., Höner zu Siederdissen, C., Tafer, H., Flamm, C., Stadler, P.F., and Hofacker, I.L. (2011). ViennaRNA Package 2.0. Algor. Mol. Biol. *6*, 1–14.
85. Martin, M. (2011). Cutadapt removes adapter sequences from high-throughput sequencing reads. EMBnet.journal *17*, 10–12.
86. Langmead, B., Trapnell, C., Pop, M., and Salzberg, S.L. (2009). Ultrafast and memory-efficient alignment of short DNA sequences to the human genome. Genome Biol. *10*, R25.
87. Li, H., Handsaker, B., Wysoker, A., Fennell, T., Ruan, J., Homer, N., Marth, G., Abecasis, G., and Durbin, R.; 1000 Genome Project Data Processing Subgroup (2009). The sequence alignment/map format and SAMtools. Bioinformatics *25*, 2078–2079.
88. Airoldi, C.A., Lugo, C.A., Wightman, R., Glover, B.J., and Robinson, S. (2021). Mechanical buckling can pattern the light-diffracting cuticle of *Hibiscus trionum*. Cell Rep. *36*, 109715.
89. Ivanov, R., Brumbarova, T., Blum, A., Jantke, A.-M., Fink-Straube, C., and Bauer, P. (2014). Sorting NEXIN1 is required for modulating the trafficking and stability of the *Arabidopsis* IRON-REGULATED TRANSPORTER1. Plant Cell *26*, 1294–1307.
90. Clough, S.J., and Bent, A.F. (1998). Floral dip: a simplified method for Agrobacterium-mediated transformation of *Arabidopsis thaliana*. Plant J. *16*, 735–743.
91. Coen, E.S., Romero, J.M., Doyle, S., Elliott, R., Murphy, G., and Carpenter, R. (1990). floricaula: a homeotic gene required for flower development in *Antirrhinum majus*. Cell *63*, 1311–1322.
92. Davidson, N.M., Hawkins, A.D.K., and Oshlack, A. (2017). SuperTranscripts: a data driven reference for analysis and visualisation of transcriptomes. Genome Biol. *18*, 148.
93. López-Gomollón, S. (2011). Detecting sRNAs by Northern blotting. In MicroRNAs in Development (Springer), pp. 25–38.

STAR★METHODS

KEY RESOURCES TABLE

REAGENT or RESOURCE	SOURCE	IDENTIFIER
Bacterial and virus strains		
Electrocompetent *Agrobacterium tumefaciens* GV3101	N/A	N/A
Chemocompetent *Escherichia coli* DH5α	N/A	N/A
Biological samples		
REDS-1: Hard Red Spring Wheat Flour Reference Material for Trace Metals and other Constituents	National Research Council, Canada	3872c082-99ae-417f-89dc-a87c46c5ae9e
Chemicals, peptides, and recombinant proteins		
Smoke Primer seed germination stimulant	Fine Bush People	N/A
Nitric acid 68% Primar Plus, for trace metal analysis	Thermo Fisher	Cat#10098862
Hydrogen peroxide 30 % (w/w), for ultratrace analysis	Merck	Cat#16911
Rhodium ICP standard, Certipure	Merck	Cat#1703450100
ICP multi-element standard solution IV	Merck	Cat#1.11355
Phosphorus, plasma standard solution, Specpure	Thermo Fisher	Cat#11301439
Glutaraldehyde	Sigma-Aldrich	Cat#G5882
Formaldehyde	Sigma-Aldrich	Cat#F8775
Sodium cacodylate	Sigma-Aldrich	Cat#C0250
Quetol 651	TAAB Laboratories	Cat#Q002
NSA	TAAB Laboratories	Cat#N010
MNA	TAAB Laboratories	Cat#M012
BDMA	TAAB Laboratories	Cat#B008
Potassium hexacyanoferrate(II) trihydrate	Sigma-Aldrich	Cat#P3289
Sodium azide	Sigma-Aldrich	Cat#71290
3,3'-diaminobenzidine tetrahydrochloride	Sigma-Aldrich	Cat#D5637
Cobalt(II) chloride hexahydrate	SLS Scientific	Cat#CHE1618
Cetrimonium bromide (CTAB)	Sigma-Aldrich	Cat#H9151
Polyvinylpyrrolidone (PVP)	Sigma-Aldrich	Cat#PVP10
RNAse A	Thermo Fisher	Cat#EN0531
SuperScript III reverse transcriptase	Thermo Fisher	Cat#18080093
Phusion Hot Start II polymerase	Thermo Fisher	Cat#F549S
Murashige & Skoog medium	Duchefa	Cat#M0222.0001
Silwet L-77	PhytoTech	Cat#S7777
DNAse I	Thermo Fisher	Cat#EN0521
Hind III	Thermo Fisher	Cat#ER0501
Pst I	Thermo Fisher	Cat#ER0612
T4 DNA ligase	Thermo Fisher	Cat#EL0014
PCRBIO Taq DNA polymerase	PCR Biosystems	Cat#PB10.11-05
5-Bromo-4-chloro-3-indolyl phosphate (BCIP)	Roche	Cat#11383221001
Nitroblue tetrazolium (NBT)	Roche	Cat#11383213001
Paraformaldehyde (PFA)	Thermo Fisher	Cat#416785000
Dextran sulphate	Thermo Fisher	Cat#BP1585-100
Bovine serum albumin (BSA)	Thermo Fisher	Cat#BP9702-100
Formamide deionized	Sigma-Aldrich	Cat#F9037-100ml
Triethanolamine	Sigma-Aldrich	Cat#90278-500ml
Proteinase K	Melford	Cat#P50220-0.025
Blocking reagent	Roche	Cat#11096176001
Tetramisole hydrochloride	Sigma-Aldrich	Cat#L9756-10G

(*Continued on next page*)

Continued

REAGENT or RESOURCE	SOURCE	IDENTIFIER
DNase I recombinant, RNase-free	Roche	Cat#4716728001
Anti-Digoxigenin-AP, Fab fragments	Roche	Cat#11093274910; RRID: AB_2734716
Eosin, 0.1%	Thermo Fisher	Cat#152880250
tRNA	Roche	Cat#10109223001
Denhardts solution, 50×	Sigma-Aldrich	Cat#D2532-5ml
Histoclear	Geneflow	Cat#A2-0105
BioScript reverse transcriptase	Meridian Bioscience	Cat#BIO-27036
T7 RNA polymerase	Roche	Cat#10881767001
DIG RNA labelling mix	Roche	Cat#11277073910
TRIzol	Thermo Fisher	Cat#15596026
T4 phosphonucleotide kinase	Thermo Fisher	Cat#EK0031
ATP, [γ-^{32}P]- 3000Ci/mmol 10mCi/ml Lead, 100 μCi	PerkinElmer	Cat#NEG002A100UC
SYBR Safe DNA gel stain	Thermo Fisher	Cat#S33102
Ultrahyb-Oligo	Ambion	Cat#AM8663
ZR small RNA ladder	Zymo	Cat#R1090
Critical commercial assays		
RNeasy plant mini kit	Qiagen	Cat#74904
RNase-Free DNase set	Qiagen	Cat#79254
Bioanalyzer RNA 6000 pico kit	Agilent	Cat#5067-1513
GenomeWalker 2.0 kit	Clontech	Cat#636405
Monarch DNA gel extraction kit	NEB	Cat#T1020S
Luna Universal qPCR master mix	NEB	Cat#M3003S
Monarch Plasmid DNA miniprep kit	NEB	Cat#T1010S
Spectrum plant total RNA kit	Merck	Cat#STRN10
Direct-zol RNA miniprep kit	Zymo	Cat#R2050
Deposited data		
Raw mRNA-seq reads	This paper	NCBI SRA: PRJNA910570
Raw small RNA-seq reads	This paper	NCBI SRA: PRJNA910570
Combined reference transcriptome	This paper	NCBI TSA: GKEE00000000
GdEXPA7 mRNA sequence	This paper	NCBI Genbank: OQ032504
GdSPL1 mRNA sequence	This paper	NCBI Genbank: OQ032505
GdmiR156 small RNA sequence	This paper	Figshare: 21750110
GdmiR162 small RNA sequence	This paper	Figshare: 21750110
Transcriptome annotations	This paper	Figshare: 21750110
Lists of differentially expressed transcripts	This paper	Figshare: 21750110
ICP-OES results	This paper	Figshare: 21750110
EXPA alignment file for phylogenetic analysis	This paper	Figshare: 21750110
Lists of differentially expressed small RNA	This paper	Figshare: 21750110
miRbase v.22	Kozomara et al.[60]	https://www.mirbase.org/ftp.shtml
Experimental models: Organisms/strains		
Gorteria diffusa: Springbok	Wild collected seed	N/A
Gorteria diffusa: Naries	Wild collected seed	N/A
Arabidopsis thaliana: Col-0	N/A	N/A
Arabidopsis thaliana: *GdEXPA7p-eGFP-N7*	This paper	N/A
Arabidopsis thaliana: *2×35S-GdSPL1*	This paper	N/A
Arabidopsis thaliana: *2×35S-GdSPL1-truncated*	This paper	N/A

(*Continued on next page*)

Continued

REAGENT or RESOURCE	SOURCE	IDENTIFIER
Oligonucleotides		
See Table S5 for Oligonucleotides	N/A	N/A
Recombinant DNA		
Plasmid: pUAP-ye	Pollak et al.[52]	N/A
Plasmid: pUAP-*eGFP*	Pollak et al.[52]	N/A
Plasmid: pUAP-*N7*	Pollak et al.[52]	N/A
Plasmid: pUAP-*GdEXPA7p*	This paper	N/A
Plasmid: pCk2-ye	Pollak et al.[52]	N/A
Plasmid: pCk1-*Hyg*^{R}	Pollak et al.[52]	N/A
Plasmid: pCk2-*GdEXPA7p-eGFP-N7*	This paper	N/A
Plasmid: pCk1-*Hyg*^{R}	Pollak et al.[52]	N/A
Plasmid: pCk3-sp	Pollak et al.[52]	N/A
Plasmid: pCk4-sp	Pollak et al.[52]	N/A
Plasmid: pCsA-*GdEXPA7p-eGFP-N7*	This paper	N/A
Plasmid: pGREEN-II-*2*×*35S*	Hellens et al.[67]	N/A
Plasmid: pGREEN-II-*2*×*35S-GdSPL1*	This paper	N/A
Plasmid: pGREEN-II-*2*×*35S-GdSPL1-truncated*	This paper	N/A
Software and algorithms		
Trimmomatic v. 0.38	Bolger et al.[68]	https://github.com/usadellab/Trimmomatic
Trinity v. 2.8.4	Grabherr et al.[69]	https://github.com/trinityrnaseq/trinityrnaseq/wiki
TransDecoder v. 5.5.0	Haas et al.[70]	https://github.com/TransDecoder/TransDecoder/wiki
Trinotate v. 3.1.1	Bryant et al.[71]	https://github.com/Trinotate/Trinotate/wiki
BUSCO v. 3.1.0	Simão et al.[72]	https://busco.ezlab.org
RSEM v. 1.3.1	Li and Dewey[73]	https://github.com/deweylab/RSEM
Bowtie v. 2.3.4.3	Langmead and Salzberg[74]	https://bowtie-bio.sourceforge.net/bowtie2/index.shtml
R v. 3.5.2	R Core Team, 2018[75]	https://www.r-project.org
tximport v. 1.10.1	Soneson et al.[76]	https://bioconductor.org/packages/release/bioc/html/tximport.html
edgeR v. 3.24.3	Robinson et al.[77]	https://bioconductor.org/packages/release/bioc/html/edgeR.html
PANTHER v. 16.0	Mi et al.[78]	http://www.pantherdb.org
MEGA v. 7	Kumar et al.[79]	https://www.megasoftware.net
ProtTest3 v. 3.4.2	Darriba et al.[80]	https://github.com/ddarriba/prottest3
MrBayes v. 3.2.6	Ronquist et al.[81]	http://nbisweden.github.io/MrBayes/download.html
ImageJ v. 1.53n	Schneider et al.[82]	https://imagej.net
blastn v. 2.4.0+	Altschul et al.[83]	https://ftp.ncbi.nlm.nih.gov/blast/executables/blast+/
RNAfold v. 2.4.18	Lorenz et al.[84]	https://www.tbi.univie.ac.at/RNA/
TrimGalore! v. 0.6.6	Martin[85]	https://github.com/FelixKrueger/TrimGalore
Bowtie v. 1.3.0	Langmead et al.[86]	https://bowtie-bio.sourceforge.net/index.shtml
SAMtools v. 1.9	Li et al.[87]	https://samtools.sourceforge.net
Other		
NanoDrop 2000 spectrophotometer	Thermo Fisher	Cat#ND-2000
2100 Bioanalyzer	Agilent	Cat#G2939BA
NovaSeq 6000 sequencer	Illumina	N/A

(*Continued on next page*)

Continued

REAGENT or RESOURCE	SOURCE	IDENTIFIER
Verios 460 scanning electron microscope	Thermo Fisher	N/A
PP3010T Cryo-SEM preparation system	Quorum	N/A
DigiTUBE, 15ml, RackLock	QMX Laboratories	Cat#QX100233
SCIMED DIGIPrep MS block	QMX Laboratories	Cat#QX100232
PlasmaQuant PQ 9000 Elite ICP-OES spectrometer	Jena Analytik	N/A
Ultracut E ultramicrotome	Leica	N/A
BX41 light microscope	Olympus	N/A
CFX384 Touch real-time PCR detection system	BioRad	Cat#1855484
M205 FA fluorescence stereomicroscope	Leica	N/A
TCS SP5 confocal microscope	Leica	N/A
ASP300 tissue processor	Leica	N/A
BX41 light microscope	Olympus	N/A
VHX-5000 digital microscope	Keyence	N/A
DNBseq-G400 sequencer	MGI Tech	N/A
15% Mini-PROTEAN TBE-Urea gel	BioRad	Cat#4566053
Hybond-NX Nylon hybridization membranes	Merck	Cat#GERPN203T
Illustra Microspin G25 columns	GE Healthcare	Cat#27-5325-01

RESOURCE AVAILABILITY

Lead contact

Further information and requests for resources and reagents should be directed to and will be fulfilled by the lead contact, Beverley Glover (bjg26@cam.ac.uk).

Materials availability

All plasmids and transgenic *Arabidopsis thaliana* lines generated in this study are available from the lead contact upon request.

Data and code availability

Raw mRNA-seq and small RNA-seq data have been deposited on NCBI SRA. The combined reference transcriptome is deposited on NCBI TSA. Sequences of *GdEXPA7* and *GdSPL1* are deposited on NCBI Genbank. All other datasets generated in this study are deposited on Figshare. All datasets generated in this study are publicly available as of the date of publication. Accession numbers are listed in the key resources table.

This paper does not report original code.

Any additional information required to reanalyze the data reported in this paper is available from the lead contact upon request.

EXPERIMENTAL MODEL AND SUBJECT DETAILS

Gorteria diffusa cultivation

Seed bearing capitula of the *G. diffusa* morphotypes Springbok and Naries were collected from two localities in Namaqualand, Northern Cape, South Africa (Springbok: 29° 41' 37.1'' S, 17° 53' 01.9'' E, Naries: 29° 44' 52.2'' S, 17° 31' 39.4'' E). Capitula were stratified with smoke primer (Cape Seed Primer, Fine Bush People, Cape Town, SA) for 24 h, and germinated in 9 × 9 cm pots with two-thirds compost (Levington's M3, Evergreen Garden Care, Nantgarw, Cardiff, UK) and one-third horticultural sand (Westland Horticulture, Dungannon, County Tyrone, UK). 12 Springbok and 12 Naries plants were selected for transcriptomic analysis, and kept in a climate chamber (16 h illumination at 150 umol/m^2/s, 20 °C, 60 % relative humidity) with watering every two-three days and no fertilisation. To enable cross-comparisons, all subsequent experiments were conducted with subsets of the same 12 Springbok and 12 Naries genotypes, which were kept alive by taking cuttings every month over the course of this study.

Arabidopsis thaliana cultivation

The *A. thaliana* lines used are listed in the key resources table. Seeds were sown in 4 × 4 cm pots with compost (Levington's M3, Evergreen Garden Care, Nantgarw, Cardiff, UK), cold stratified at 4°C for 4 d, and kept in a climate chamber (16 h illumination at 150 umol/m^2/s, 20 °C, 60 % relative humidity) with daily watering and no fertilisation.

METHOD DETAILS

Transcriptome assembly and annotation

Three types of developing *G. diffusa* ray florets (spotted and unspotted ray florets from the same Springbok flower buds as well as spotted ray florets from Naries flower buds) with a length of two to three mm each were collected from each genotype. Florets were snap frozen in liquid N_2 and ground to powder using a tissue lyser (Retsch Technology, DE). Total RNA was extracted with a Qiagen RNeasy plant mini kit (Qiagen, NL) including on-column DNAse treatment according to the manufacturer's protocol. RNA was quantified on a NanoDrop 2000 (Thermo Fisher Scientific, Massachusetts), and RNA integrity was determined on 1.5% agarose gels and on a 2100 Bioanalyzer (Agilent Technologies, USA). Samples were paired-end-sequenced by Novogene, UK with 150 bp read length on an Illumina NovaSeq 6000 sequencer (Illumina, USA) to a depth of 20 + 20 M reads per sample. Demultiplexed mRNA-seq reads were quality filtered using *Trimmomatic* v. 0.38[68] with the settings ILLUMINACLIP:TruSeq3-PE-2.fa:2:30:10 LEADING:5 TRAILING:5 SLIDINGWINDOW:4:5 MINLEN:25. A combined reference transcriptome was assembled with *Trinity* v. 2.8.4[69] using trimmed reads from spotted and unspotted ray florets of Springbok plant 8, and from spotted ray florets of Naries plant 13. Coding regions were predicted with *TransDecoder* v. 5.5.0,[70] and annotated with *Trinotate* v. 3.1.1[71] against the SwissProt, Pfam, SignalP, EggNOG, Kegg, and Gene Ontology databases. Finally, transcriptome completeness was estimated with *BUSCO* v. 3.1.0[72] using the lineage database eudicotyledons_odb10.

Gene expression and overrepresentation test

Trimmed reads from all samples were mapped to the combined reference transcriptome, and expression levels were estimated using *RSEM* v. 1.3.1[73] with *Bowtie* v. 2.3.4.3[74] as aligner. Posterior mean counts were extracted in *R* v. 3.5.2[75] using the *R* library *tximport* v. 1.10.1,[76] and transcripts with fewer than 5 counts per M reads in at least 12 samples were removed. To find genes underlying petal spot development, a negative binomial generalised linear model was fitted for reads with at least a 1.5 fold expression difference between spotted and unspotted Springbok petals, accounting for the paired experimental design with samples coming from the same individual. Differential expression was then determined with a quasi-likelihood F-test. To further isolate genes underlying Springbok-specific petal spot traits, gene expression differences between spotted Springbok and spotted Naries petals were first determined with a standard negative binomial generalised linear model fitted for reads with at least a 1.5 fold expression difference, and a quasi-likelihood F-test. Results of both analyses were then filtered for transcripts differentially expressed both between spotted and unspotted Springbok ray florets, and between spotted Springbok and Naries ray florets. All analyses were conducted using the *R* library *edgeR* v. 3.24.3.[77] Transcripts with a significant expression difference were annotated using the blastx results of the reference transcriptome annotation. In cases where annotation differed between isoforms of a gene, the annotation matching the isoform(s) with the total most mapped reads was chosen for the gene. Lists of both putative general and Springbok-specific petal spot genes were submitted to *PANTHER* v. 16.0[78] to retrieve gene ontology (GO) IDs from the GO annotation dataset 'GO biological process complete' (released 18.08.2020). A *PANTHER* binomial overrepresentation test with FDR correction (released 04.07.2020) was then performed for both gene lists using a list of all genes included in the differential expression analysis as reference.

CryoSEM imaging

Cryo-Scanning Electron Microscopy (Cryo-SEM) and cryo-fracture imaging of developing *G. diffusa* ray florets was conducted according to Airoldi et al. (2021)[88] on a Verios 460 scanning electron microscope (Thermo Fisher Scientific, USA) equipped with a Quorum PP3010T cryo-apparatus.

ICP-OES

Spotted entire ray florets, unspotted entire ray florets, the dark-coloured base of spotted ray florets and the orange-coloured tip of spotted ray florets from four Springbok genotypes (plants 8, 10, 14, and 20) were harvested and dried at 50°C for 72 h. For each genotype, 0.1 g of dry tissue was incubated with 2 ml nitric acid (69% w/v) and 0.5 ml hydrogen peroxide (30% w/v) at 95°C for 16 h. Samples were diluted with milliQ water to contain 5.5% nitric acid, and 0.1 ug g^{-1} Rhodium was added as internal standard. The concentrations of Fe, Mn and Zn were measured on a PlasmaQuant PQ 9000 Elite instrument (Jena Analytik, DE). Calibration was performed using 0, 0.025, 0.05, 0.1, 0.2, 0.4, 0.6, 0.8 and 1 $\mu g\ g^{-1}$ standards of Fe, Mn and Zn. Hard red spring wheat reference material (National Research Council (Canada) was treated in the same manner and analysed in the same run.

Perls'-DAB staining and microscopy

Fully developed petal spots of Springbok plant 8 were dissected with a razor blade, separating the dark papillate area in narrow strips. Samples were fixed in 2% glutaraldehyde / 2% formaldehyde in 0.05 M sodium cacodylate buffer (pH 7.4) containing 2 mM $CaCl_2$ overnight at 4°C. Samples were washed 2× in 0.05 M NaCAC buffer and 2× in DIW. Samples were then dehydrated in an ethanol series (50% / 70% / 95% / 100% / 100 % dry) and embedded in Quetol resin by exchanging the resin mix once a day for 5 days. The Quetol resin mixture is: 12 g Quetol 651, 15.7 g NSA, 5.7 g MNA and 0.5 g BDMA (all from TAAB Laboratories Equipment Ltd, UK). The resin was cured by incubating at 60°C for 48 h. Sections with a thickness of 1 μm were prepared using a diamond histoknife in a Leica Ultracut E ultramicrotome and placed on superfrost microscope slides. DAB staining was performed according to Ivanov et al.[89] In brief, samples were first stained in Perls' staining solution (2% (w/v) $K_4Fe(Cn)_6$, 2% (w/v) HCl) at RT under 500 mbar vacuum for 1 h. Stained samples were washed three times with ddH_2O, incubated for 1 h in DAB preparation solution (0.1 M NaN_3 and 0.3% (w/v)

H_2O_2 in MeOH), and washed again three times in 0.1 M phosphate buffer. Samples were then vertically incubated in intensification solution (0.025% 3,3′-diaminobenzidine tetrahydrochloride (DAB), 0.005% H_2O_2, and 0.005% $CoCl_2$ in 0.1 M phosphate buffer) at 20°C for 5 min, and washed three times with ddH_2O. DAB-stained samples were imaged under an Olympus BX41 light microscope at 4-40× magnification.

Phylogenetic analysis of *GdEXPA7*

Coding sequences of *Arabidopsis thaliana EXPA1-18* and *20-25*, and *Helianthus annuus EXPA1, 4* and *6-11* were downloaded from GenBank and aligned manually at protein level with *GdEXPA1, 7* and *15* using *MEGA* v. 7.[79] Amino acid sequences of the two conserved *expansin* domains[48] were extracted and loaded into *ProtTest3* v. 3.4.2[80] to determine the best-fit model of amino acid replacement. A phylogenetic gene tree was constructed with *MrBayes* v. 3.2.6[81] using LG + Γ as evolutionary model. The run was stopped when apparent stationary of *log*-likelihood was reached (2 million generations with a sampling frequency of 500 and a diagnosis frequency of 5000).

Analysis of *GdEXPA7* promoter sequence

Young leaves of Springbok plant 8 were snap frozen in liquid N_2 and ground to powder using a tissue lyser (Retsch Technology, Germany). DNA was extracted using a modified cetrimonium bromide (CTAB) protocol: CTAB extraction buffer (2% w/v CTAB and 1% w/v PVP in 1.4 M NaCl, 20 mM EDTA and 100 mM Tris-HCl) was added to the samples at a ratio of 5 μl / mg tissue. Samples were vortexed, incubated in a 60°C water bath for 30 min, and centrifuged at 14000 × *g* and 20°C for 5 min. The supernatant was transferred to a 1.5 ml tube, 5 μl RNAse A (Thermo Fisher Scientific, USA) was added, and samples were incubated at 32°C for 15 min. An equal volume of chloroform: isoamylalcohol (1:1) was added, samples were vortexed for 5 s, and centrifuged at 14000 × *g* and 20°C for 1 min. The upper, aqueous phase was transferred to a 1.5 ml tube, 0.7 volume of isopropanol were added to the sample, and DNA was precipitated by incubation at -20°C for 15 min. The sample was centrifuged at 14000 × *g* and 20°C for 10 min, the supernatant decanted, and the pellet washed with cold 70% EtOH. The DNA pellet was then dried for 1 min and dissolved in 25 μl dH_2O. The *GdEXPA7* promoter sequence was amplified from this sample using a Universal GenomeWalker 2.0 kit (Clontech Laboratories, USA) according to the manufacturer's protocol. In brief, four DNA libraries were produced by digesting 1 μg DNA each with DraI, EcoRV, PvuII, and StuI. DNA libraries were purified using a NucleoSpin Gel and PCR Clean-Up kit (Macherey-Nagel, Germany), and ligated to GenomeWalker adaptors. Two PCRs were conducted with these libraries; a primary PCR with primers AP1 and *GdEXPA7*-GSP1, and a secondary, nested PCR with primers AP2 and *GdEXPA7*-GSP2 (Table S5). Amplified libraries were analysed on a 1.5% agarose/EtBr gel, and three PCR fragments of ca. 350 bp, 1 kb and 2 kb length were excised and purified with a Monarch DNA Gel Extraction kit (New England Biolabs, UK) according to the manufacturer's protocol. PCR fragments were Sanger-sequenced using primers AP2 and *GdEXPA7*-GSP2, and the sequence inspected for conserved root hair-specific *cis*-elements.[51]

RT-qPCR of *GdEXPA7* in *G. diffusa* tissues

Four different types of young, developing tissues (spotted ray florets, unspotted ray florets, roots and leaves) were collected from eight *G. diffusa* genotypes (plants 3, 6, 8, 14, 16, 17, 19, 20). Total RNA was extracted from these tissues and subjected to on-column DNAse treatment as described above. RNA aliquots of 1 μg were digested a second time with DNAse I (Thermo Fisher Scientific, USA), and reverse transcribed to cDNA with SuperScript III reverse transcriptase (Thermo Fisher Scientific, USA) according to the manufacturer's protocols. Intron-spanning primer pairs of the reference genes *actin 1* (*GdACT1*), *elongation factor 2* (*GdEF2*) and *ubiquitin-conjugating enzyme E2 10* (*GdUBC10*, Table S5) were tested for lack of dimerization and amplification stability across all tissues and different template concentrations (Figure S3) Reverse transcription quantitative real-time PCR (RT-qPCR) was performed in triplicate on a CFX384 Touch™ Real-Time PCR Detection System (BioRad Laboratories, USA) using *GdEF2* and *GdUBC10* as reference genes; PCR: 0.25 μl *GdEXPA7*-RTqPCR-F and *GdEXPA7*-RTqPCR-R primer (10 μM, Table S5), 5 μl Luna® Universal qPCR Master Mix (2×, New England Biolabs, UK), 1 μl cDNA (congruent to 10 ng input RNA), 3.5 μl ddH2O; PCR conditions: 95°C for 1 min, 40 cycles of (95°C for 15s, 60°C / plate readout for 30 s). Relative expression of *GdEXPA7* was calculated using the ΔΔCt algorithm, and expression differences between groups were determined in *R* v. 3.5.2 with ANOVA and Tukey HSD *post-hoc* tests.

Cloning of *GdEXPA7* promoter reporter plasmid

To assess *GdEXPA7* promoter activity in different tissues, a Loop level two construct[52] was assembled containing an *eGFP-N7* nuclear-localised reporter gene driven by the *GdEXPA7* promoter. A 773 bp fragment upstream of the *GdEXPA7* start codon was amplified from genomic DNA of Springbok plant 8 using Phusion Hot Start II polymerase (Thermo Fisher Scientific, USA); PCR: 4 μl HF buffer (5×), 0.4 μl dNTPs (10 mM each), 2 μl *GdEXPA7p*-F/R primers (5 μM each, Table S5), 0.2 μl polymerase, 1 μl gDNA, 10.4 μl ddH_2O; PCR conditions: 98°C for 30 s, 35 cycles of (98°C for 10 s, 59°C for 30 s, 72°C for 30 s), 72°C for 5 min. A 1:50 dilution of PCR product was used as template for a secondary PCR with the same conditions, but using *Loop-GdEXPA7p-F/R* primers (5 μM each, Table S5). The PCR product was analysed on a 1.5% agarose/EtBr gel, and an 813 bp fragment was excised and purified with a Monarch DNA Gel Extraction kit (New England Biolabs, UK) according to the manufacturer's protocol. The purified *GdEXPA7* promoter was cloned into a Loop level 0 vector (pUAP-ye) according to Pollak et al.,[52] and chemo-competent *Escherichia coli* DH5α were transformed with this construct using a standard heat-shock protocol. The plasmid was extracted with a Monarch Plasmid DNA Miniprep kit (New England Biolabs, UK) according to the manufacturer's protocol, and Sanger-sequenced using primers UAP-F/R (Table S5). Next, a loop level 1 plasmid (pCk2-*GdEXPA7p-eGFP-N7*) was assembled according to Pollak et al.[52] using the plasmids

pUAP-*GdEXPA7p*, pUAP-*eGFP*, pUAP-*N7* and the backbone plasmid pCk2-ye. The assembled plasmid was transferred to *E. coli* DH5α and extracted as above, and Sanger-sequenced using the primers PC-F/R (Table S5). The pCk2-*GdEXPA7p-eGFP-N7* plasmid was combined with a pCk1-*Hyg*^{R} plant hygromycin resistance plasmid and the two spacer plasmids pCk3-sp and pCk4-sp in a pCsA-ye Loop level 2 backbone to the final pCsA-*GdEXPA7p-eGFP-N7* construct according to Pollak et al.[52] The assembled plasmid was again transferred to *E. coli* DH5α and extracted as above, and then Sanger-sequenced using the primers PC-F/R and *GdEXPA7p*-F (Table S5).

Localisation of *GdEXPA7* promoter activity

Wild-type *Arabidopsis thaliana* Col-0 plants were grown from seeds as described above. Developing inflorescences were cut back to the rosette after primary bolts appeared on most plants. After 7 weeks, plants were transformed with the pCsA-*GdEXPA7p-eGFP-N7* construct using floral dip as described in Clough and Bent[90] with some modifications: Electro-competent *Agrobacterium tumefaciens* GV3101 were transformed with the pCsA-*GdEXPA7p-eGFP-N7* construct using a standard electroporation protocol. After 24 h incubation at 28°C / 180 rpm in 20 ml lysogeny broth (LB) medium with 50 μg ml^{-1} spectinomycin, 25 μg ml^{-1} gentamicin and 50 μg ml^{-1} rifampicin, the culture was diluted 1:25 in 250 ml LB medium with the same concentration of antibiotics, and incubated at 28°C / 180 rpm for 12 h. 125 ml culture was centrifuged at 5000 × *g* and 20°C for 10 min, and the pellet resuspended in 250 ml infiltration medium (50 g l^{-1} Sucrose with 2.3 g l^{-1} vitamin containing Murashige & Skoog medium (MS, Duchefa Biochemie, NL) and 0.03% Silwet L-77 at pH 6.0). Open flowers were removed and aboveground tissues were submerged in this solution for 30 s. Inoculated plants were placed horizontally in covered trays for 24 h and then kept as before until seed ripening. Seeds were sterilised in 10% sodium hypochlorite, washed three times with ddH_2O, and sown in petri dishes with 2.2 g l^{-1} MS medium, 10 g l^{-1} Sucrose and 50 μg ml^{-1} hygromycin in 0.8% plant agar. Plates were kept in the dark at 4°C for 4 d, and then under 16 h illumination at 150 umol/m^2/s at 20 °C. Surviving seedlings were transferred to soil and kept under the same conditions as the parent plants until seed ripening. Sowing was repeated as above, and surviving plants were examined under a fluorescence stereomicroscope (Leica M205 FA) and a confocal microscope (Leica TCS SP5) 15 d and 32 d after germination.

Angle measurements of *G. diffusa* ray florets

Standardised top-view photos of single flowers from 54 wild *G. diffusa* Springbok individuals were taken in Namaqualand, Northern Cape, South Africa (29° 40' 34.9" S, 17° 48' 50.7" E) using a Nikon D90 DLSR camera connected to a custom-built clamp. Angles between spotted ray florets were determined on these images using the angle measurement tool in ImageJ v. 1.53n.[82] First, the innermost / oldest spotted ray floret was identified, and the angles to adjacent spotted ray florets were then measured in counter-clockwise direction.

GdSPL1 expression in *A. thaliana*

A 1 μg aliquot of total RNA from Springbok plant 8 (see above) was digested with DNAse I (Thermo Fisher Scientific, USA), and reverse transcribed to cDNA with SuperScript III reverse transcriptase (Thermo Fisher Scientific, USA) according to the manufacturer's protocols. Full *GdSPL* coding sequence (444 bp) as well as a truncated variant with a premature stop codon (333 bp) were PCR amplified using Phusion Hot Start II polymerase (Thermo Fisher Scientific, USA); PCR: 4 μl HF buffer (5×), 0.4 μl dNTPs (10 mM each), 2 μl *Hind*III-*GdSPL1*-F primer (5 μM, Table S5), 2 μl *Pst*I-*GdSPL1*-R/Rs primer (5 μM, Table S5), 0.2 μl polymerase, 1 μl cDNA, 10.4 μl ddH_2O; PCR conditions: 98°C for 30 s, 35 cycles of (98°C for 10 s, 61.2°C for 30 s, 72°C for 30 s), 72°C for 5 min. The corresponding band was purified from agarose gel (see above), digested with *Hind* III and *Pst* I (Thermo Fisher Scientific, USA), and ligated into a pGREEN-II-*2×35S* overexpression vector[67] using T4 DNA ligase (Thermo Fisher Scientific, USA) according to the manufacturer's protocols. Chemo-competent *E. coli* DH5α were transformed with these constructs using a standard protocol, the plasmids were extracted with a Monarch Plasmid DNA Miniprep kit (New England Biolabs, UK) according to the manufacturer's protocol, and Sanger-sequenced using primers *GdSPL1*-F and *GdSPL*1-R/Rs (Table S5). Wild-type *A. thaliana* Col-0 plants were transformed with both constructs using floral dip as described above, but replacing spectinomycin with 50 μg ml^{-1} kanamycin. Seeds of transformed plants were sown on MS + sucrose medium with 50 μg ml^{-1} kanamycin, and surviving seedlings were transferred to soil as described above. Eight transformed plants were grown in a climate chamber (see above) together with one plant transformed with the short construct and eight wild-type *A. thaliana* Col-0 plants. For each plant, the number of rosette leaves was determined at bolting stage (Figure S4), and leaf tissue was collected in liquid N_2. Total RNA was extracted, DNAse I digested and reverse transcribed as described above. Semi-quantitative PCR was conducted for all nine transformed and one wild-type plant using PCRBIO Taq DNA Polymerase (PCR Biosystems, UK); PCR: 5 μl PCRBIO buffer (5×), 1 μl *GdSPL1*-F and 1 μl *GdSPL1*-R/Rs primer (10 μM each, Table S5), 0.5 μl polymerase, 1 μl cDNA (congruent to 10 ng input RNA), 16.5 μl ddH_2O; PCR conditions: 95°C for 1 min, 40 cycles of (95°C for 15 s, 57°C for 15 s, 72°C for 15 s), taking out 5 μl reaction after 30 and 35 cycles. Samples were analysed on a 1.5% agarose / EtBr gel.

In-situ hybridisation of *GdSPL1*

G. diffusa flower buds of 20 mm size from both Springbok plant 8 and Naries plant 13 were fixed in 4% paraformaldehyde solution. Fixed material was dehydrated using a series of increasing ethanol concentrations without NaCl and embedded in Paraplast plus (Merck KGaA, DE) in an ASP300 tissue processor (Leica Biosystems, DE). Embedded tissue was sectioned to 8 μm width and hybridized according to Coen et al.[91] with slight modifications. Protease treatment was performed with Proteinase K (1 μg/mL in

100 mM Tris, pH 7.5, and 50 mM EDTA) at room temperature for 10 min, instead of Pronase. The post-hybridization washes were performed in 0.1× SSC. After the colour reaction, slides were mounted in 30% glycerol and photographed using both an Olympus BX41 light microscope and a Keyence VHX-5000 microscope (Keyence Ltd., UK). All hybridization experiments were repeated three times.

To produce *in-situ* probes, flower buds of 20 mm size from Springbok plant 8 were harvested and Total RNA was extracted using a Spectrum plant total RNA kit (Merck KGaA, DE). Reverse transcription was performed using BioScript reverse transcriptase (Meridian Bioscience, USA) for 45 min at 42°C with oligo-dT primers, and the generated cDNA was used as template for both antisense and sense GdSPL1 probe preparation. A T7 promoter sequence was included both in the reverse primer of the antisense probe, and in the forward primer of the sense probe (Table S5). *In vitro* transcription was performed with T7 RNA polymerase (Roche AG, CH) and DIG RNA Labeling Mix (Roche AG, CH) was used for RNA labelling with digoxigenin-UTP. Probes were not hydrolysed.

Detection and folding of *pri-GdmiR156*

The reverse complement of the *miR156* binding site, situated within the 3'-UTR of the *GdSPL1* gene (TGACAGAAGAGAGAGAGCAT) was searched against the combined Springbok and Naries reference transcriptome (see above) with *blastn* v. 2.4.0+[83] using the option '-task blastn-short'. Transcripts, which (1) contained fewer than two mismatches to the query sequence, (2) were differentially expressed between spotted and unspotted Springbok petals, and (3) had no annotated ORF were kept for further analysis. Candidate transcripts were pruned to 10 bp upstream and downstream of the miR156 binding site, and minimum free energy folding structures were predicted using *RNAfold* v. 2.4.18 from the *ViennaRNA Package 2.0*.[84]

Differential expression analysis of small RNA

Samples for small RNA sequencing were prepared for spotted and unspotted ray florets of Springbok plant 6, 8, 17 and 20 with the same tissue used for mRNA-seq (see above). Total RNA was extracted from 10 mg ground tissue using a Direct-zol RNA miniprep kit (Zymo Research, USA) including on-column DNAse treatment according to the manufacturer's protocol. RNA was quantified on a NanoDrop 2000 (Thermo Fisher Scientific, Massachusetts), and RNA integrity was determined on 1.5% agarose gels and on a 2100 Bioanalyzer (Agilent Technologies, USA). Unique Molecular Identifier (UMI) small RNA-seq libraries were prepared from these samples. Libraries were single-end-sequenced by BGI Genomics, PRC with 50 bp read length on an MGI DNBseq-G400 sequencer (MGI Tech, PRC) to a depth of 10 M reads per sample. Demultiplexed small RNA-seq reads were quality filtered using *TrimGalore*! v. 0.6.6[85] with the settings '–quality 20 –small_rna –max_length 35 –length 16'. In a first step, the combined mRNA-seq transcriptome assembly (see above) was collapsed to SuperTranscripts[92] with *Trinity* v. 2.8.4,[69] and the trimmed small RNA-seq reads were aligned to the SuperTranscripts using *Bowtie* v. 1.3.0[86] with the settings ' -n 0 -l 10 -m 100 -k 1 –best –strata'. In a second step, the trimmed small RNA-seq reads were aligned to the complete mature miRNA database from miRbase v.22[60] using *Bowtie* v. 1.3.0[86] with the settings '-n 1 -l 10 -m 100 -k 1 –best –strata'. Both alignments were analysed independently as follows: Posterior mean counts were extracted into *R* v. 3.5.2[75] with *SAMtools* v. 1.9[87] and custom scripts, and transcripts with fewer than 40 total counts were removed. A negative binomial generalised linear model was fitted for reads with at least a 1.5 fold expression difference between spotted and unspotted Springbok petals, accounting for the paired experimental design with samples coming from the same individual. Differential expression was then determined with a quasi-likelihood F-test. All analyses were conducted using the *R* library *edgeR* v. 3.24.3.[77]

Northern blotting of *GdmiR156* and *GdmiR162*

Total RNA for Northern blotting was extracted from spotted and unspotted ray florets of Springbok plant 6, 8 and 20 using a Direct-zol RNA miniprep kit (Zymo Research, USA) as described above, with the same tissue used for mRNA-seq and small RNA-seq (see above). Northern blot analysis was conducted as described in López-Gomollón.[93] In brief, 6 μg of total RNA was separated in a 15% denaturing polyacrylamide gel (BioRad Laboratories, USA), blotted to Hybond NX membranes (Amersham BioSciences, UK) and UV crosslinked. Expression of small RNAs was assessed by hybridisation to a gamma [P32]-labelled (PerkinElmer, USA) nucleic acid oligonucleotide probe and exposure. SybrGold staining was used to assess equal loading. ZR small RNA ladder (Zymo Research, USA) was used to size the bands. Probe sequences are provided in Table S5.

QUANTIFICATION AND STATISTICAL ANALYSIS

Gene ontology analyses were conducted in *PANTHER* v. 16.0,[78] phylogenetic analyses were conducted in MrBayes v. 3.2.6,[81] and all other statistical analyses were conducted in *R* v. 3.5.2.[75] Statistical tests used, sample sizes (n) and their representations, and definitions of center, dispersion and precision measures of each experiment are described in the corresponding figure legends and method details sections. Significance was defined as p-value < 0.05.